



Position control of a quadcopter drone using evolutionary algorithms-based self-tuning for first-order Takagi–Sugeno–Kang fuzzy logic autopilots

Edwar Yazid ^{a,*}, Matthew Garratt ^b, Fendy Santoso ^b

^a Research Center for Electrical Power and Mechatronics, Indonesian Institute of Sciences, Indonesia

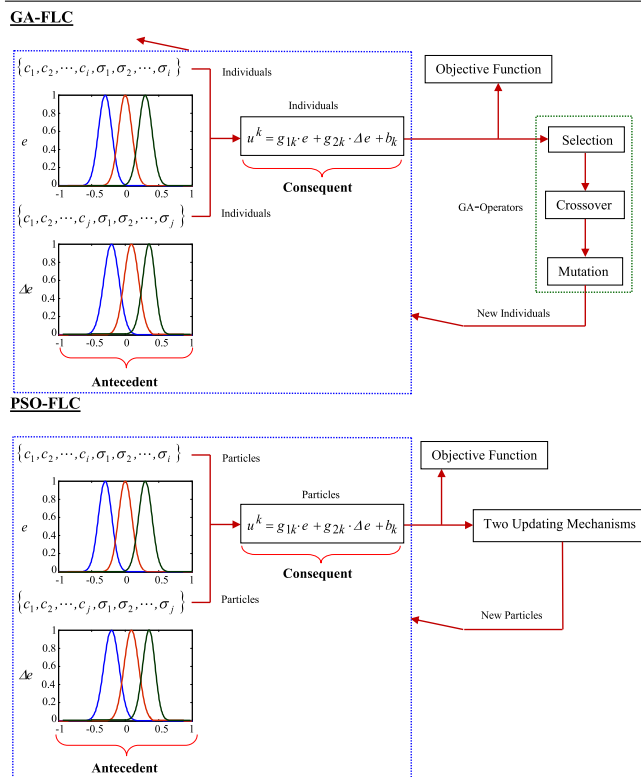
^b School of Engineering and Information Technology, University of New South Wales, Australia



HIGHLIGHTS

- Evolutionary algorithms-based self-tuning for first-order Takagi–Sugeno–Kang fuzzy logic autopilots are proposed. The proposed controllers are applied for position control of quadcopter drone, which is a multi-input multi-output (MIMO) system, with highly non-linear rigid body dynamics and severe cross-couplings.
- Given constant and varying step functions, ABC-FLC has slower rise and peak time, and faster settling time in the absence of overshoots. On the contrary, GA-FLC with a mutation rate of 0.1 has faster rise time and bigger overshoots compared to GA-FLC with a mutation rate of 0.4 and PSO-FLC.
- Given constant and varying step functions, all proposed controllers yield ununiformity in the shape and position of the fuzzy sets although there are overlap zones among several tuned fuzzy sets. However, under sine function, ABC-FLC yields uniformity in the shape of fuzzy sets, and the overlap zone is almost fifty percent.
- Overall, all three-dimensional control surfaces appear to have the same tendency, which is nonlinear and the volume of ABC-FLC is smaller than the other controllers. However, under constant and varying step functions, the shapes of control surface of ABC-FLC has less distinctive small bumps in the plane

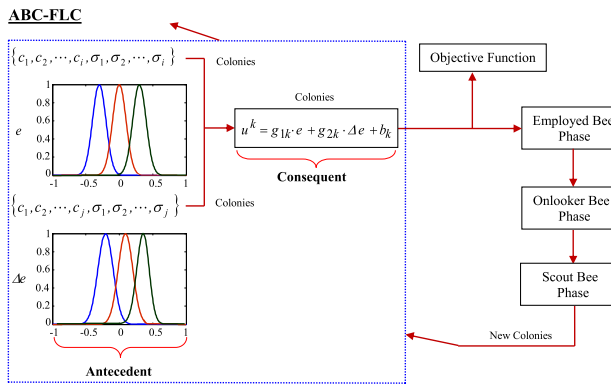
GRAPHICAL ABSTRACT



* Corresponding author.

E-mail address: edwar.putra@gmail.com (E. Yazid).

of e and Δe , while under sine function, ABC-FLC has distinctive smaller bumps compared to other controllers.



ARTICLE INFO

Article history:

Received 13 February 2017
Received in revised form 16 July 2018
Accepted 13 February 2019
Available online 19 February 2019

Keywords:

Quadcopter drone
Takagi-Sugeno-Kang
FLC
Evolutionary algorithms

ABSTRACT

Trajectory tracking control of a quadcopter drone is a challenging work due to highly-nonlinear dynamics of the system, coupled with uncertainties in the flight environment (e.g. unpredictable wind gusts, measurement noise, modelling errors, etc). This paper addresses the aforementioned research challenges by proposing evolutionary algorithms-based self-tuning for first-order Takagi-Sugeno-Kang-type fuzzy logic controller (FLC). We consider three major state-of-the-art optimisation algorithms, namely, Genetic Algorithm, Particle Swarm Optimisation, and Artificial Bee Colony to facilitate automatic tuning. The effectiveness of the proposed control schemes is tested and compared under several different flight conditions, such as, constant, varying step and sine functions. The results show that the ABC-FLC outperforms the GA-FLC and PSO-FLC in terms of minimising the settling time in the absence of overshoots.

© 2019 Elsevier B.V. All rights reserved.

1. Introduction

The concept of the fuzzy sets was introduced by Prof Lotfi A. Zadeh in 1965 [1]. Ever since, it has been widely used by researchers either for fundamental and applied researches or industry oriented applications. For control application, fuzzy sets concept has been introduced as intelligent controller by Mamdani [2] and Takagi, Sugeno, and Kang [3,4]. The Takagi-Sugeno-Kang (T-S-K)-type fuzzy model has advantages over the Mamdani-type counterpart in terms of computationally efficiency, making the system works well with optimization and adaptive techniques [5,6]. Its application has crossed over many engineering fields, e.g. in the form of intelligent controller [5–16], modeling and system identification techniques [17–22]. However, the main challenge of employing this type of fuzzy model is to have appropriate fuzzy parameters to achieve good performance and robustness. Manual tuning of such parameters is indeed not an amenable solution, especially for a multi-input, multi-output system. It may not lead to an optimum performance despite being time-consuming. Tuning process also becomes more difficult when the parameters of the control system are coupled, time-dependent, and nonlinear. This condition suggests the development of simple optimization mechanisms, that can rapidly converge.

Genetic algorithms (GA), particle swarm optimization (PSO), and artificial bee colony (ABC) are subsets of the evolutionary algorithms which have been applied for many engineering problems. However, evolutionary algorithms-based self-tuning for the T-S-K-type fuzzy model is relatively new. Efforts have been devoted by several researchers to fine tune the fuzzy parameters for different applications. For instance, Shun et al. [7] enhanced the learning ability and the robustness of sliding mode controller by combining with the first-order T-S-K-type fuzzy model. Their contribution was to optimise the coefficients of fuzzy rules of the consequence. Their control strategy was implemented to a switched reluctance motor direct torque control drive system.

Anupam and Vijay [8] incorporated the first-order T-S-K-type fuzzy model with a fractional PID-type controller to overcome the uncertainties in the system models. The ABC-GA was introduced to tune the fuzzy parameters, and applied numerically in some benchmark plants. Smoczek and Szpytko [9] implemented the GA technique to tune the parameters of the zero-order T-S-K-type fuzzy model (parameters of triangular-shaped membership functions). Their proposed controller was applied for an anti-sway crane control system. Ilyes et al. [11] introduced kernel ridge regression to tune the parameters of the first-order T-S-K-type fuzzy model, and applied the system to control a surge tank and continuous stirred tank reactor. Nemanja et al. [16] applied the PSO algorithm to tune the parameters of the zero-order T-S-K-type fuzzy model (fuzzy sets) and combined with the LQR controller for controlling the smart composite beams. Radu et al. [18] developed a new class of T-S-K-type fuzzy model for modeling and system identification of anti-lock braking systems. The fuzzy rule consequence is in the form of state-space models. They applied simulated annealing (SA) and PSO algorithms to tune the fuzzy rule antecedent.

With regard to a quadcopter drone, it is known that the system has an efficient and effective airframe configuration over traditional helicopters of a similar size. This type of robotic aircraft does not require swash plates to constantly vary the blade angle during rotation. Quadcopter drone also produces the same overall thrust although the diameter of each blade is smaller than similar sized helicopter. The system can be classified as a multi-input multi-output (MIMO) system, with highly nonlinear rigid body dynamics and severe cross-couplings among loops, making the control design process a rather challenging task. Thus the modeling process and control design become challenging tasks. Researches with regard to a specific application of FLC in the area of modeling and control of quadcopter drones are still very limited as reported in the literatures. For instance, Santoso et al. [23] proposed the use of FLC-based self-tuning autopilot for the AR. Drone quadcopter to achieve better transient response. Their

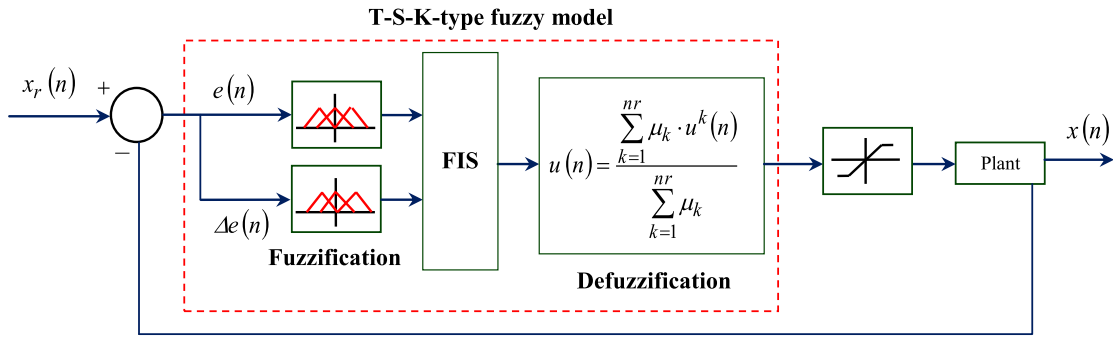


Fig. 1. Closed-loop control system of a T-S-K-type FLC.

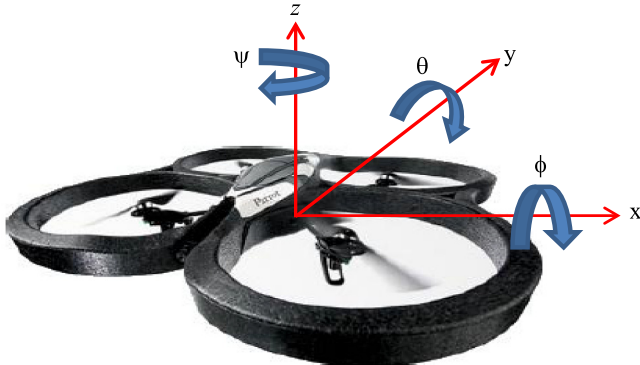


Fig. 2. Quadcopter drone as a plant.

results showed that the implementation of the FLC to facilitate automatic tuning on PD control leads to a better performance.

Based on the aforementioned discussion, evolutionary algorithms are proposed to tune the first-order T-S-K-type FLC's antecedent and consequent parameters, and applied for control position of a quadcopter drone. Three evolutionary algorithms, namely, genetic algorithm (GA), particle swarm optimization (PSO), and artificial bee colony (ABC) algorithms are implemented to optimise the performance of the first-order T-S-K-type FLC. The proposed controllers are named as GA-FLC, PSO-FLC, and ABC-FLC. The effectiveness of the three proposed controllers is tested and comprehensively compared under multiple flight conditions. To the best of our knowledge, this research has not been reported in the literature.

The rest of this paper is organized as follows. Section 2 describes the control design and the problem formulation of the system. Section 3 presents the concept of optimization for the first-order T-S-K-type FLC via evolutionary algorithms. Section 4 discusses the experimental setup of proposed controllers. Section 5 presents our results. Finally, Section 6 concludes this paper.

2. Closed-loop control system of a quadcopter drone under the first-order Takagi–Sugeno–Kang-type fuzzy logic controller (FLC)

A typical structure of a T-S-K-type FLC in a discrete closed-loop control system with a quadcopter drone as the plant is depicted in Figs. 1 and 2, respectively. Let say, x and x_r denote the actual and reference longitudinal positions of the drone in discrete time index n , respectively, then the position error e and the error derivation Δe can be calculated by,

$$e(n) = x_r(n) - x(n), \quad (1a)$$

$$\Delta e(n) = x_r(n) - x(n-1). \quad (1b)$$

Variables e and Δe become inputs in T-S-K-type fuzzy model, which consist of three basic components namely fuzzification, fuzzy inference system (FIS, rule base for decision logic), and defuzzification. The earlier is a process to convert each element of input data to degrees of membership by a lookup in certain membership functions.

If both inputs are taken as the input vector $z = \{e_i \ \Delta e_j\}$ and modeled by Gaussian membership functions, then the degrees of membership can be computed as follows,

$$\mu_{ij}(z) = \exp\left(\frac{-(z - c_{ij})^2}{\sigma_{ij}^2}\right), \quad i = 1, \dots, ne, \quad j = 1, \dots, nde. \quad (2)$$

Eq. (2) contains parameters c and σ , which determine the location and the shape of the fuzzy set, respectively. Gaussian membership function is chosen because of its smooth function, and it has only two parameters to quantify the membership function. This clearly gives advantage to the number of parameters to be optimized and expedites the optimization process. Notations ne and nde indicate the number of fuzzy sets of both inputs. If the input space of e and Δe is mapped into a number of fuzzy linguistic terms such as N (Negative), Z (Zero), and P (Positive) as shown in the first block of Fig. 1, then the fuzzy logic operators must be applied for both inputs. In the FIS, fuzzy operators such as AND or OR connect both inputs to become an antecedent, and since the first-order T-S-K-type fuzzy model is employed, then the output in the consequent is in the form of a linear equation which is a function of e and Δe values. Antecedent and consequent form the k th IF-THEN rules, where $k = 1, \dots, nr$ and they are expressed in Eq. (3),

$$\text{Rule } k: \underbrace{\text{If } e_i(n) \text{ is } (N, Z, P) \text{ and } \Delta e_j(n) \text{ is } (N, Z, P)}_{\text{Antecedent}} \text{ then } \underbrace{u^k(n) = p_{g1k} \cdot e_i(n) + g_{2k} \cdot \Delta e_j(n) + b_k}_{\text{Consequent}}. \quad (3)$$

Coefficients in the consequent are parameters g_{1k}, g_{2k} and b_k , and they become the gains for FLC (fuzzy gains). Index nr indicates the number of rules (multiplication between ne and nde). Eq. (3) calls for two remarks:

1. If the constant b_k is set up to be zero, then Eq. (3) is equivalent with nonlinear gain scheduling PD controller with different variable gains in different regions of input space.
2. If variables g_{1k} and g_{2k} are taken to be zero, then the output is constant, $u^k(n) = b_k$, and fuzzy model becomes zero-order T-S-K-type FLC.

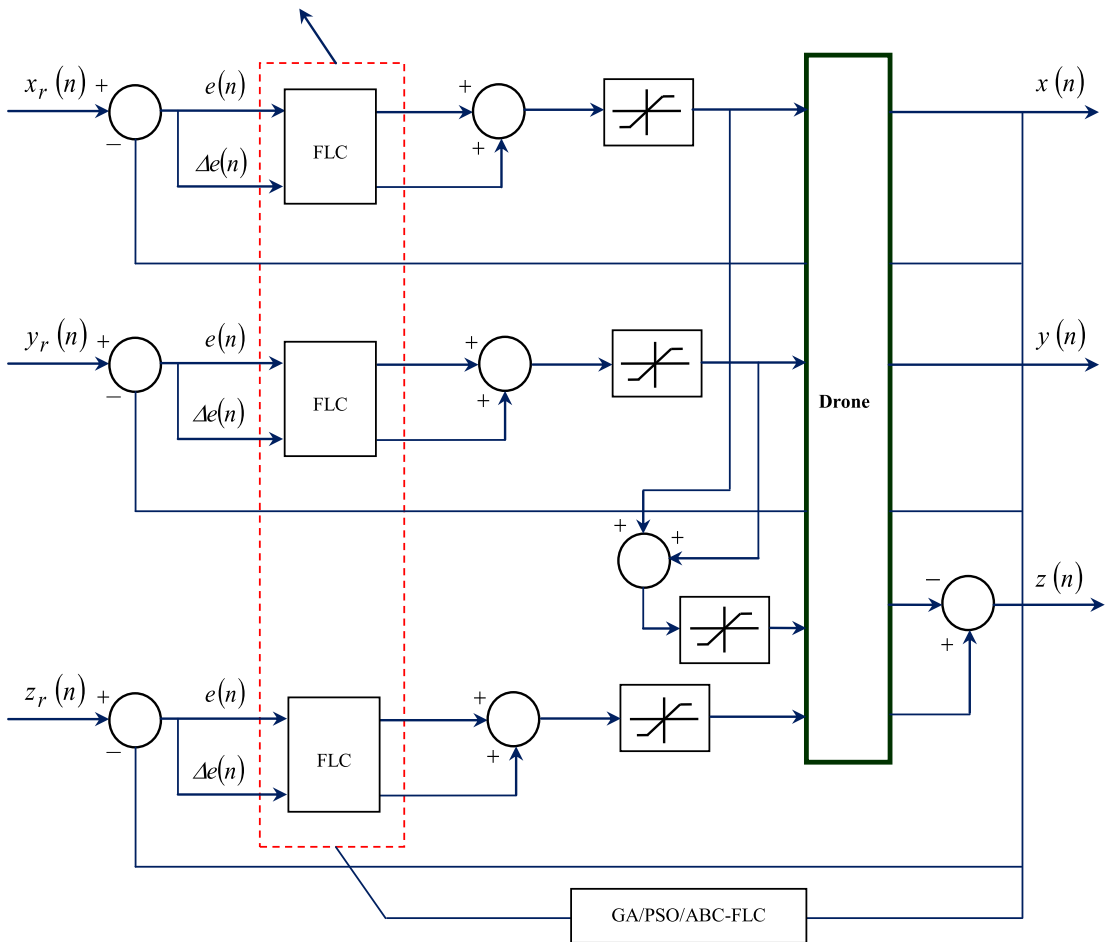


Fig. 3. Details of the first-order T-S-K-type FLC parameters optimization for a quadcopter drone.

It is worthy to note that the higher-order T-S-K-type fuzzy models are possible to be employed. However, they introduce significant complexity with increasing the processing time of control actions as an expense.

All rules built from the knowledge of the designer are evaluated in parallel using fuzzy reasoning in the FIS as shown in the second block of Fig. 1. The results of the rules are combined and defuzzified as shown in the third block of Fig. 1. A crisp output is obtained by using weighted average defuzzification method as given by Eq. (4a),

$$\mu_k = \text{AND} (\mu_i(z_1), \mu_j(z_2)), \quad (4a)$$

$$u(n) = \frac{\sum_{k=1}^{nr} \mu_k \cdot u^k(n)}{\sum_{k=1}^{nr} \mu_k}. \quad (4b)$$

Term μ_k is firing degree of k th rules in the interval $[0, 1]$ and they are from the antecedents of Eq. (3). Eqs. (2)–(3) suggest that in one fuzzy rule, the first-order T-S-K-type FLC contains two parameters as membership parameters of fuzzy set in the antecedent and three parameters as fuzzy gains in the consequent. They are named as fuzzy parameters $\{c, \sigma, g_{1k}, g_{2k}, b_k\}$. The first two terms indicate to the membership functions of the fuzzy sets in the antecedent while the rest indicates the gains of FLC. The five parameters are designed to match the actual longitudinal position of the drone $x(n)$ with the reference longitudinal position $x_r(n)$ by giving a corrective action in terms of control action $u(n)$. Under any types of system input, the control action fully depends on the five parameters, and they significantly affect the

control performance. Suboptimal parameters lead to the system becomes unstable, high overshoots and large steady-state error. Hence, evolutionary algorithms are employed to optimize those parameters.

3. Self-tuning for first-order T-S-K-type FLC through evolutionary algorithms

Fuzzy parameters $\{c, \sigma, g_{1k}, g_{2k}, b_k\}$ are modeled as individuals in the GA, as particles in the PSO and as colonies in the ABC. The optimization process of these parameters with underlying plant is depicted in Figs. 3–5. For the sake of clarity, optimizers for the parameters of FLC using GA, PSO and ABC are called GA-FLC, PSO-FLC and ABC-FLC, respectively hereafter. The major phases of these algorithms are outlined in the next section. If there is ne fuzzy sets in e and nde fuzzy sets in Δe then the parameters are $s = \{c_1, c_2, \dots, c_i, \sigma_1, \sigma_2, \dots, \sigma_i, g_{1k}, g_{2k}, b_k\}$. The total number of parameters to be optimized is calculated as follows,

$$L = (2 \cdot ne) + (2 \cdot nde) + (3 \cdot nu). \quad (5)$$

Eq. (5) is applicable only for Gaussian membership function, where a constant of 2 refers to number of parameters in Eq. (2), a constant of 3 refers to number of parameters in the consequent of Eq. (3) under a number of sets of u . As an example, if fuzzy set of e is three and fuzzy set of Δe is three then the number of fuzzy gains in u is nine. Hence, the total number of parameters to be optimized is twenty-one. GA-FLC, PSO-FLC and ABC-FLC optimize the twenty one parameters and control the underlying system at

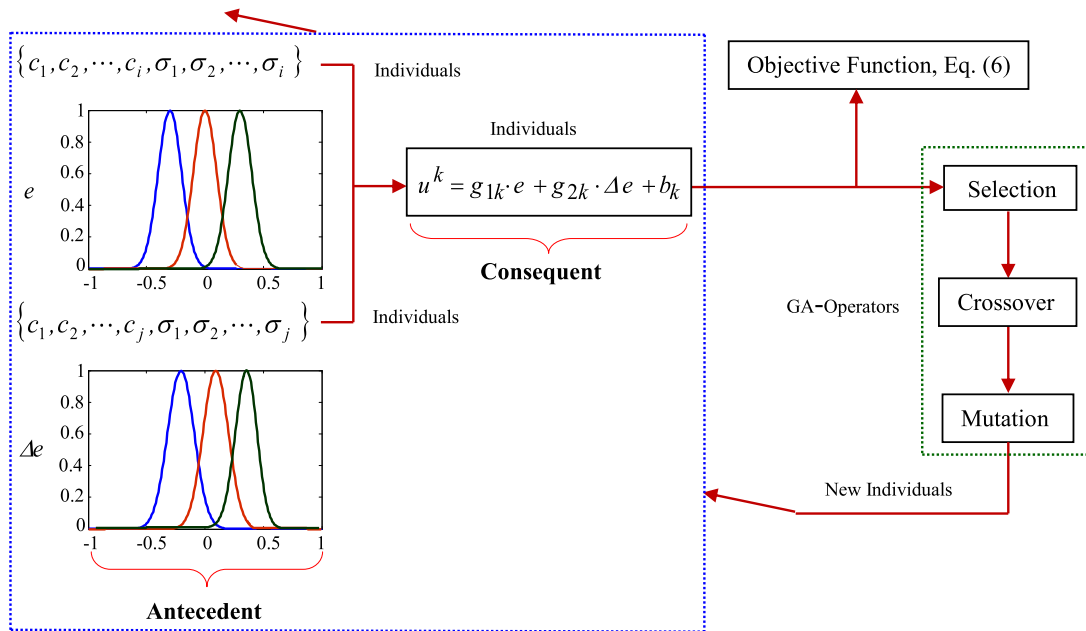


Fig. 4. Parameters optimization process in GA-FLC.

the same time according to Figs. 3–5. In some cases, parameter b can be ignored so that the total number of parameters in Eq. (5) can be reduced.

3.1. Objective function

GA-FLC, PSO-FLC and ABC-FLC require an objective function in order to select the best solutions for new individuals, particles and foods, respectively. Various objective functions based on error performance criterion can be selected to evaluate the performance of these controllers. Each objective function is fundamentally the same unless the specific error performance criterion is specified with regard to the case at hand. In this paper, a sum square error (SSE) is chosen as the objective function to determine the cost function for each solution by calculating the square of the difference between the reference position and the actual position obtained by from the proposed controllers. This objective function is regarded to be sufficient for controlling the position of quadcopter drone. Since all controllers are assigned to control the position in x (longitudinal)-, y (lateral)- and z (vertical)-directions, then the objective function is defined as a summation of SSE of each controller as written by Eq. (6),

$$\text{SSE} = \sum_{n=1}^N (x_r(n) - x(n))^2 + \sum_{n=1}^N (y_r(n) - y(n))^2 + \sum_{n=1}^N (z_r(n) - z(n))^2. \quad (6)$$

Terms in Eq. (6) are as follows: N is the number of data, $x(n)$, $y(n)$, $z(n)$ are the actual positions in x-, y- and z-directions, respectively while $x_r(n)$, $y_r(n)$, $z_r(n)$ are the reference positions in respective directions.

3.2. GA-Fuzzy logic controller (GA-FLC)

In GA-FLC, individuals which represent the first-order T-S-K-type FLC parameters are collected in a population of $s = \{c_1, c_2, \dots, c_i, \sigma_1, \sigma_2, \dots, \sigma_i, c_1, c_2, \dots, c_j, \sigma_1, \sigma_2, \dots, \sigma_j, g_{1k}, g_{2k}, b_k\}$. Their

initial values are generated randomly within predefined search boundaries using Eq. (7),

$$s_{i,j} = s_j^{\min} + \lambda (s_j^{\max} - s_j^{\min}), \quad i = 1, \dots, S, \\ j = 1, \dots, L. \quad (7)$$

Terms in Eq. (7) can be explained as follows: $s_{i,j}$ is j th individuals of i th populations, s_j^{\min} and s_j^{\max} are lower and upper bounds of j th individuals, respectively, λ is a random number in range of $[0, 1]$, S is the number of populations, and L is the number of the first-order T-S-K-type FLC parameters. Each individual is then evaluated based on the objective function in Eq. (6) and expressed in terms of cost function. Selection, crossover and mutation as GA operators are then applied to select the individuals with the best performance to enable the crossover and mutation operators to generate the new population (offspring).

After the GA operators are applied, a new population with evolved individuals is produced. If the optimal individuals are not obtained, then the iteration process continues until the stopping criterion is satisfied. The number of iterations or convergence can be the stopping criterion. Selection of the values and the types of operators of selection, crossover and mutation depend on the dynamic behavior of the underlying system. Elitism, roulette wheel and ranking selection can be selection operators, while arithmetic as well as uniform and nonuniform can be crossover and mutation operators, respectively [24]. In summary, the optimization process employed in the GA-FLC is depicted in Fig. 4.

3.3. PSO-Fuzzy logic controller (PSO-FLC)

In PSO-FLC, the first-order T-S-K-type FLC parameters, $s = \{c_1, c_2, \dots, c_i, \sigma_1, \sigma_2, \dots, \sigma_i, c_1, c_2, \dots, c_j, \sigma_1, \sigma_2, \dots, \sigma_j, g_{1k}, g_{2k}, b_k\}$ are called as particles. These particles have initial velocity and position. Particles are evaluated by using objective function in Eq. (6), where particles with the highest cost value is stored as p_{best} , whereas the particles with the lowest cost value is taken as g_{best} . The lowest cost value indicates the current closest particle's position to the target. The goal of the PSO algorithm is to accelerate each particle in the highest cost value toward the lowest cost value in each iteration by increasing its velocity. In order to achieve this goal, the velocity and position of each

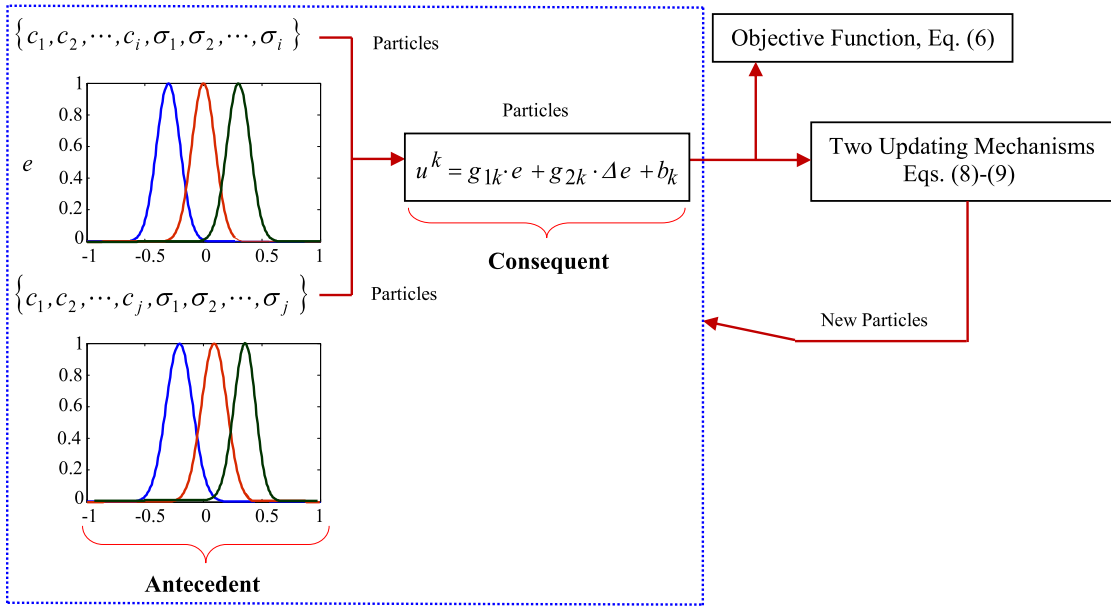


Fig. 5. Parameters optimization process in PSO-FLC.

particle must be updated using two updating mechanisms as in Eqs. (8)–(9) [25,26]. The lowest cost value changes only when any particle's with the highest cost value comes closer to the target than the lowest cost value. With iteration, the lowest cost value gradually moves closer to the target until one of the particles reaches the target. The optimization process employed in the PSO-FLC is depicted in Fig. 5.

$$v_{i,j} = C (w \cdot v_{i,j} + c_1 r_1 (p_{best\ i,j} - s_{i,j}) + c_2 r_2 (g_{best\ i} - s_{i,j})) , \quad i = 1, \dots, S, \quad j = 1, \dots, L \quad (8)$$

$$s_{i,j} = s_{i,j} + v_{i,j}. \quad (9)$$

Eqs. (8)–(9) contain parameters are as follows: $s_{i,j}$ and $v_{i,j}$ denote the i th position and velocity components of the j th particle, respectively. Eq. (8) contains four constants C , w , c_1 and c_2 which are set by the algorithm designer. Constant C is a constriction factor, w is the inertia weight which balances the local and the global searches, c_1 is the cognition parameter and c_2 is the social parameter. The terms r_1 and r_2 are two random numbers uniformly selected from the interval $[0, 1]$. Values of four constants C , w , c_1 and c_2 must be chosen in order such that control response for the quadcopter drone has minimal settling time in the absent of overshoot.

3.4. ABC-Fuzzy logic controller (ABC-FLC)

The first-order T-S-K-type FLC parameters, $s = \{c_1, c_2, \dots, c_i, \sigma_1, \sigma_2, \dots, \sigma_j, c_1, c_2, \dots, c_j, \sigma_1, \sigma_2, \dots, \sigma_j, g_{1k}, g_{2k}, b_k\}$ are called as colonies in the ABC-FLC. The major phases of this algorithm comprise initialization, employed bee, onlooker bee and scout bee phases. Step by step of optimization process above is depicted in Fig. 6. Due to lengthy expressions, details about the ABC algorithm can be read in references [25]. Similar with GA-FLC and PSO-FLC, the number of employed bee, onlooker and scout must be chosen properly.

Based on block diagram in Fig. 3 and descriptions in Figs. 4–6, following algorithm is proposed:

- (1) Assign the parameters:

- (a) The number of particles and generations as well as values for three constants c_0 , c_1 , c_2 and two terms r_1 and r_2 for PSO.
- (b) The number of populations and generations as well as values for selection, crossover and mutation rates for GA.
- (c) The number of colony sizes and generations as well as values of onlooker number, employed bee number and scout number for ABC.

- (2) Initialize the values of individuals, particles and colonies randomly via Eq. (7). The values become input for the FLC. The output of FLC is a cost function sse , calculated via Eq. (6) and the estimated fuzzy parameters $s = \{c_1, c_2, \dots, c_i, \sigma_1, \sigma_2, \dots, \sigma_j, c_1, c_2, \dots, c_j, \sigma_1, \sigma_2, \dots, \sigma_j, g_{1k}, g_{2k}, b_k\}$.
- (3) The cost function in step (2) is minimized using the PSO, GA and ABC by optimizing the fuzzy parameters $s = \{c_1, c_2, \dots, c_i, \sigma_1, \sigma_2, \dots, \sigma_j, c_1, c_2, \dots, c_j, \sigma_1, \sigma_2, \dots, \sigma_j, g_{1k}, g_{2k}, b_k\}$.
- (4) Step (2) and (3) are iterated until a convergence is achieved, and the cost function is obtained.

It is worthy to note that the same procedure described above has so far only been developed for Gaussian membership function. The same principle can be applied if other membership functions are used, but the corresponding number of parameters which characterize the membership function must be modified according to Eq. (5).

4. Experimental setup

Experimental setup for implementing the proposed control algorithms is shown in Fig. 7. Four types of sensors are embedded in the drone: a three-axis MEMS accelerometer for measuring lateral accelerations, a one and two-axis gyro for measuring angular accelerations, two ultrasonic sensors for measuring altitude and a downward facing camera for velocity estimation. The four rotors are driven by four brushless DC motors. Sensors acquisition, image processing, state estimation and closed-loop control are executed by a 40 MHz PIC and a 468 MHz ARM9-core processor run a LINUX-based Robot Operating System (ROS) with Wi-Fi communications to a ground computer. Flight tests were

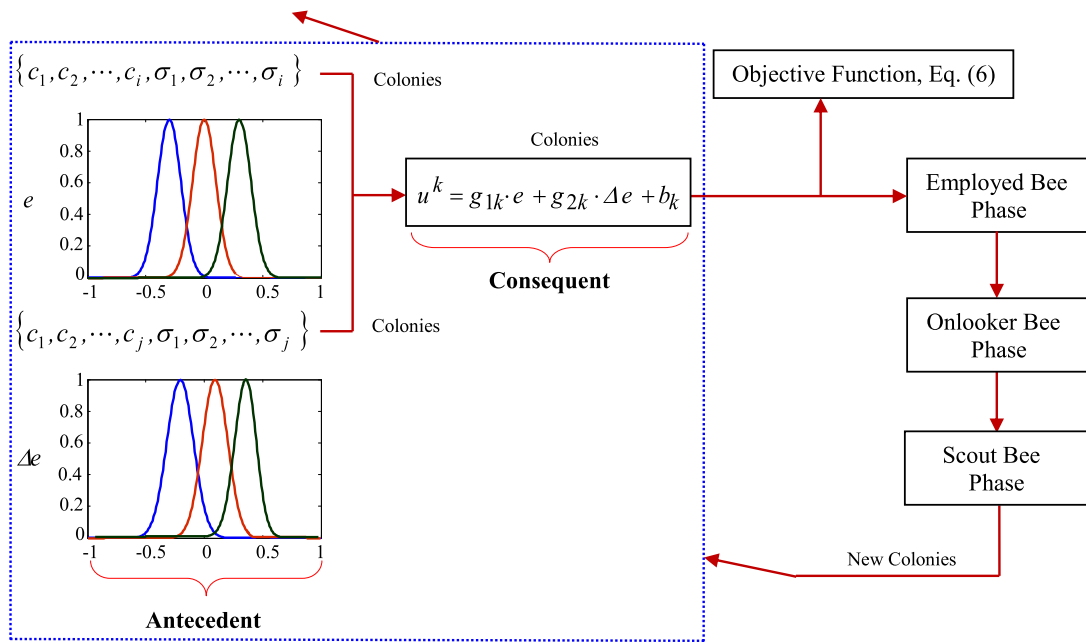


Fig. 6. Parameters optimization process in ABC-FLC.

conducted in the UAV laboratory, University of New South Wales, Australia.

Two controllers must be utilized to control the position and the attitude in terms of two control loops. The inner loop is for attitude control $\{\varphi \theta \psi\}$ while the outer loop is for position control $\{x y z\}$. This is illustrated in a diagram block as shown in Fig. 8. The inputs for brushless DC motor as actuators are given in terms of $\{\Delta\omega_F \Delta\omega_\varphi \Delta\omega_\theta \Delta\omega_\psi\}$ and cause vertical, roll, pitch and yaw motions, respectively. The relationship between the inputs for motor and the angular speed of the rotors is given as follows [19],

$$\begin{aligned} \Delta\omega_F + \omega_h &= \frac{1}{4} (\omega_1 + \omega_2 + \omega_3 + \omega_4), \\ \Delta\omega_\varphi &= \frac{1}{2} (\omega_2 - \omega_4), \\ \Delta\omega_\theta &= \frac{1}{2} (\omega_3 + \omega_1), \quad \Delta\omega_\psi = \frac{1}{4} (\omega_1 - \omega_2 + \omega_3 - \omega_4). \end{aligned} \quad (10)$$

Terms in Eq. (10) can be explained as follows: $\Delta\omega_F$ denotes the angular speed to maintain hover, $\Delta\omega_h$ is the rotation due to vertical movement and $\Delta\omega_{\varphi,\theta,\psi}$ denotes motor rotations causing roll, pitch and yaw motion, respectively while ω_i , $i = 1, 2, 3, 4$ corresponds to the individual motor of the drone. For safety reasons, the autopilot for the attitude control has been carefully designed by the manufacturer so that it is not made adjustable from the end-user and only the outer loop can be easily reprogrammed under the Robotic Operating System (ROS).

5. Experimental results

In this section, performance of the proposed GA-FLC, PSO-FLC and ABC-FLC are investigated under three cases. First case is position control under constant step function, second case is under varying step function, and the last case is sine function. Parameters used in the GA-FLC are given by 50 individuals in population size of 0.1 for a low mutation rate, and 0.4 for a hyper-mutation rate with a selection rate of 0.5, and a crossover rate of 0.65. Selection operator is elitism with elite number per generation of 1 while the crossover operator is arithmetic. For the

PSO-FLC, it uses 50 individuals in population size of 1 for a constriction factor, 0.9 for inertia weight, while cognitive and social parameters are set at 2. For ABC-FLC, the number of colonies is set at 50 while the number of onlooker and employed bee equals to the half of the colony size, and scout bee is set at 1. Details are summarized in Table 1. It should be noted that values of parameters in Table 1 are considered as the best parameters for the system obtained after several runs. All controllers are executed in 50 iterations with the intervals of search area are $-2 \leq x \leq 2$ for $\{c_1, c_2, \dots, c_i, \sigma_1, \sigma_2, \dots, \sigma_j, c_1, c_2, \dots, c_j, \sigma_1, \sigma_2, \dots, \sigma_j\}$ and $0 \leq x \leq 300$ for p_{1k}, p_{2k}, b_k . Control performances in time domain are assessed in terms of rise time, settling time, overshoots and peak time and compared. Due to the lengthy results, only control results in x -direction are displayed in this paper since the trend is similar for the y - and z -directions. The number of fuzzy sets for error and error derivative is set into three, namely negative (N), zero (Z) and positive (P), respectively. Membership function utilized is Gaussian function which is characterized by two parameters as expressed in Eq. (2). By having six fuzzy sets in total, The number of parameters to be optimized in the antecedent is twelve as indicated by Eq. (5).

Since the number of fuzzy sets of error and the error derivative is set into three, then the number of rules becomes nine as tabulated in Table 2. As such, there are nine gains to be optimized in the consequent as indicated in Eq. (5). Hence, total variables to be optimized become twenty one. It should be noted that the rules are generated intuitively, and fixed during the optimization process. Optimization is then performed simultaneously for the twenty one variables. In order to ensure that the comparisons are unbiased, the initial parameters of the twenty one variables are initiated similarly in all optimization algorithms.

5.1. Position control under constant step function

A unit step as a reference position signal at $t = 0$ for $x_r = 1$ m is sent to the drone as the first task, and the result is $x \rightarrow 1$ m. Actual position of the drone in x -direction with respect to reference position is shown in Fig. 9(a). For clarity, time window of 0–3 s is displayed in Fig. 9(b). From the figures, it is seen that the drone is able to track the reference position, and all

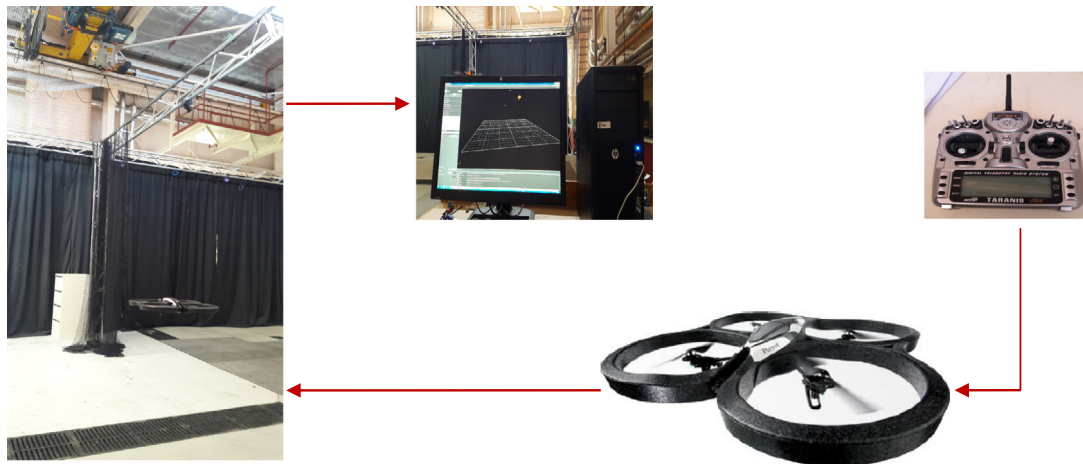


Fig. 7. Experimental setup of a quadcopter drone.

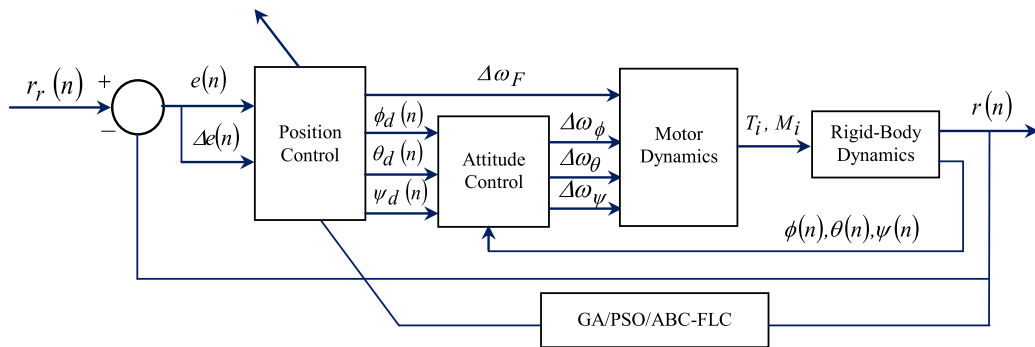


Fig. 8. Diagram block of proposed control system.

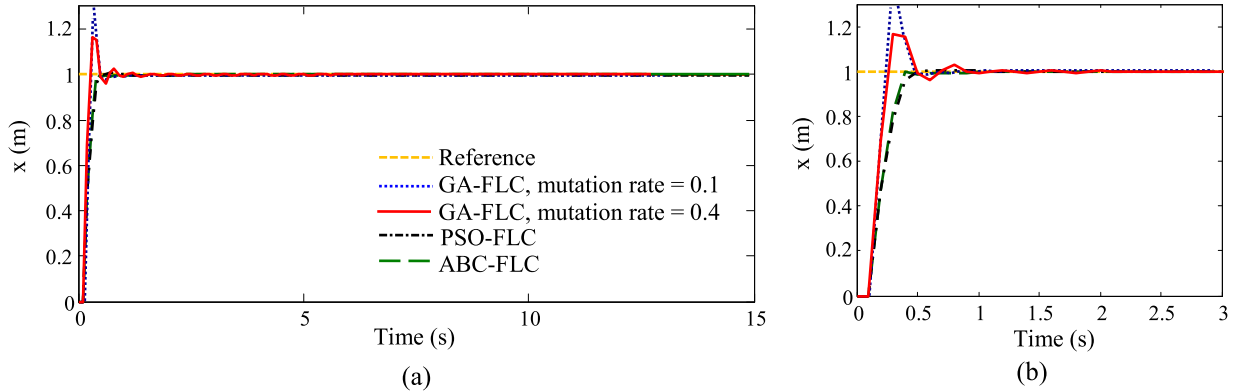


Fig. 9. Drone responses for step function in x -direction (a) time window of 0–15 s (b) time window of 0–3 s.

Table 1
Parameters of GA, PSO and ABC.

| GA | | | |
|--------------------------------|----|---|-------------------|
| Number of iterations | 50 | Selection rate | 0.5 |
| Number of populations | 50 | Crossover rate | 0.65 |
| Number of optimized parameters | 21 | Mutation rate | 0.1 & 0.4 |
| PSO | | | |
| Number of iterations | 50 | Constriction factor, C | 1 |
| Number of particles | 50 | Cognition and social parameters, c_1, c_2 | 2 |
| Number of optimized parameters | 21 | Inertia weight, w | 0.9 |
| ABC | | | |
| Number of iterations | 50 | Onlooker number | 50% of the colony |
| Number of colonies | 50 | Employed bee number | 50% of the colony |
| Number of optimized parameters | 21 | Scout number | 1 |

Table 3
Controller performance under step function.

| Performance | GA-FLC Mutation rate = 0.1 | | GA-FLC Mutation rate = 0.4 | | PSO-FLC | | ABC-FLC |
|-------------------|-------------------------------|--|-------------------------------|--|---------|--|---------|
| Rise time (s) | 0.12 | | 0.11 | | 0.24 | | 0.22 |
| Settling time (s) | 0.82 | | 0.48 | | 0.44 | | 0.38 |
| Overshoot (%) | 10.58 | | 1.43 | | 0.81 | | 0 |
| Peak time (s) | 0.3 | | 0.3 | | 0.7 | | 0.8 |

Table 4
Optimal parameters of membership functions of e under step function.

| Parameters | Fuzzy set | GA-FLC Mutation rate = 0.1 | | GA-FLC Mutation rate = 0.4 | | PSO-FLC | | ABC-FLC | |
|------------|-----------|-------------------------------|-------|-------------------------------|-------|---------|-------|---------|-------|
| | | Initial | Tuned | Initial | Tuned | Initial | Tuned | Initial | Tuned |
| σ | N | 0.52 | 0.23 | 0.52 | 0.12 | 0.52 | 0.08 | 0.52 | 0.6 |
| c | | 0.17 | -1.21 | 0.17 | -0.40 | 0.17 | -0.6 | 0.17 | -0.2 |
| σ | Z | 0.19 | 0.20 | 0.19 | 0.08 | 0.19 | 0.17 | 0.19 | 0.25 |
| c | | 0.007 | 0.01 | 0.007 | -0.01 | 0.007 | 0.01 | 0.007 | 0.03 |
| σ | P | 0.05 | 0.11 | 0.05 | 0.12 | 0.05 | 0.5 | 0.05 | 0.31 |
| c | | -0.88 | 1.23 | -0.88 | 0.41 | -0.88 | 0.9 | -0.88 | 0.20 |

Table 5
Optimal parameters of membership functions of Δe under step function.

| Parameters | Fuzzy set | GA-FLC Mutation rate = 0.1 | | GA-FLC Mutation rate = 0.4 | | PSO-FLC | | ABC-FLC | |
|------------|-----------|-------------------------------|-------|-------------------------------|-------|---------|-------|---------|-------|
| | | Initial | Tuned | Initial | Tuned | Initial | Tuned | Initial | Tuned |
| σ | N | 0.33 | 0.12 | 0.33 | 0.12 | 0.33 | 0.08 | 0.33 | 0.6 |
| c | | 0.26 | -1.06 | 0.26 | -0.3 | 0.26 | -0.12 | 0.26 | -0.4 |
| σ | Z | 0.89 | 0.22 | 0.89 | 0.10 | 0.89 | 0.51 | 0.89 | 0.4 |
| c | | 0.35 | 0.41 | 0.35 | 0.01 | 0.35 | 0.01 | 0.35 | 0.01 |
| σ | P | 0.68 | 0.12 | 0.68 | 0.12 | 0.68 | 0.08 | 0.68 | 0.03 |
| c | | 0.39 | 1.05 | 0.39 | 0.13 | 0.39 | 0.71 | 0.39 | 0.91 |

Table 2
Fuzzy rules for GA-FLC, PSO-FLC and ABC-FLC.

| Error | Error derivative | Δe_x | | |
|-------|------------------|--------------|---|---|
| | | | | |
| | | N | Z | P |
| e_x | N | P | P | N |
| | Z | Z | Z | Z |
| | P | P | N | N |

controllers have successfully stabilized it with respect to time. Performance of each controller is summarized in Table 3. By observing Fig. 9 and Table 3, it can be found out that during the tracking process, the GA-FLC with mutation rates of 0.1 and 0.4 result in overshoots of 10.58% and 1.43% to the drone on the way to its steady-state condition, respectively. Superiority of the hyper-mutation GA method over the low mutation GA method is reported in the previous researches [25,26]. On the contrary, PSO-FLC results in smaller overshoots than the GA-FLC, where it is about 0.81%. However, the ABC-FLC has the best performance among the others in the absence of overshoots. Performance in the absence of overshoots is also followed by resulting the fastest settling time among the others. Superiority of the ABC over the PSO and the GA is also reported in the previous research [26].

Although the GA-FLC results in overshoots, Table 3 shows that the GA-FLC for both mutation rates gives faster rise time than the ABC-FLC and the PSO-FLC. The values are almost an half from the latter under this task. The fast rise time of the GA-FLC is the reason behind the overshoots occurrence. Fast rise time that creates the overshoots may lead to the slow settling time. Further, the value of rise time closely relates with the value of the gains of the controller. With regard to this fact, optimal gains of all controllers are tabulated in Table 6 to see the relationship. It is

found that the optimal gains of the ABC-FLC are mostly lower than the other controllers. This confirms why the ABC-FLC has slower rise and peak time, and faster settling time in the absence of overshoots. However, controller with minimal overshoots is favorable in the drone flight control.

Cost functions resulted by each controller in optimizing all parameters of the first-order T-S-K-type FLC are depicted in Fig. 10(a). It can be observed that the cost functions of PSO-FLC and GA-FLC with a mutation rate of 0.4 start to converge after the-2nd iteration, after the-6th iteration for the ABC-FLC, and after the-41st iteration for the GA-FLC with a mutation rate of 0.1. Although the ABC-FLC has slower convergence than the PSO-FLC, however, as the number of iterations increases, cost function of ABC-FLC is getting lower than the PSO-FLC until each converges into certain values (after the-33rd iteration). In the other side, the GA-FLC with a mutation rate of 0.1 shows a premature convergence until it evolves at the-41st iteration. Results in Fig. 10 suggest that the ABC-FLC outperforms the GA-FLC and the PSO-FLC, and also confirm the performance of each controller in Fig. 9.

To support the results in Figs. 9–10, convergence histories of the fuzzy sets of e and Δe of ABC-FLC under step function are presented in Figs. 11–12. The values of c and σ are largely scattered in the initial iterations (first column of Fig. 11). It leads to the condition that the shape and position of the fuzzy sets are ununiform. As the number of iterations increases (second column of Fig. 11), values of c and σ are getting converged, the shape and position of the fuzzy sets are getting localized in certain values. In the convergence history (after the-33rd iteration), values of c and σ have converged, and the fuzzy sets have localized in respective values (third column of Fig. 11). However, ABC-FLC yields nonuniformity in the shape and position of the fuzzy sets although there are overlap zones among several tuned fuzzy sets.

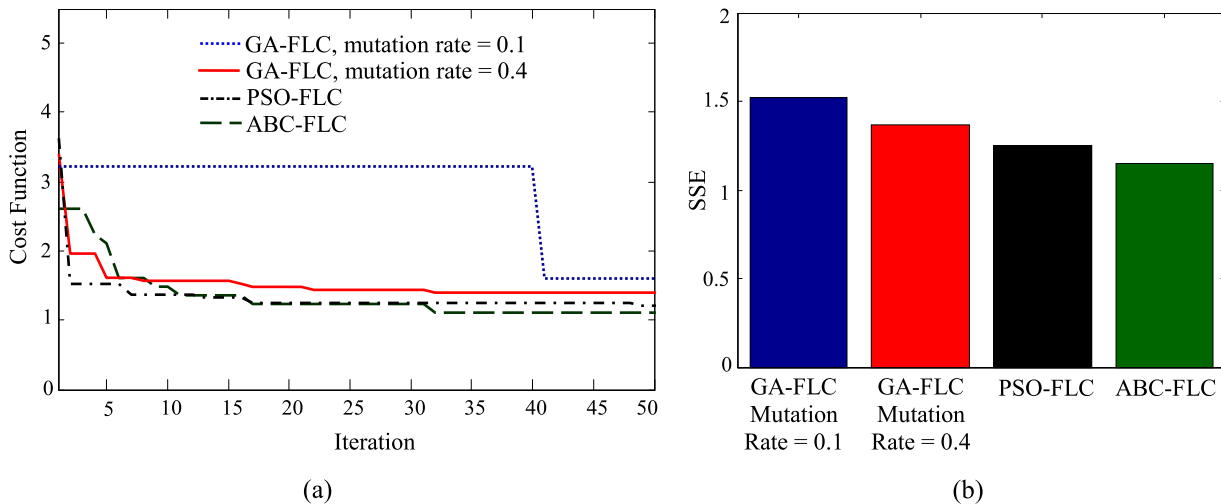


Fig. 10. Cost functions for step function in x -direction (a) cost functions with respect to number of iterations (b) SSE.

For clarity of Fig. 11, the initial and optimized values of fuzzy sets, and the controller gains are summarized in Tables 4–6.

Data in Tables 4–6 are then plotted to form the three-dimensional control surface of each controller which relates u , e and Δe under fuzzy rules in Table 2. Surface of each controller is depicted in Fig. 13, where it is found that the control surfaces tuned from control algorithms are much different from the initial control surface. Those figures suggest that the control surface is affected significantly by the values of tuned fuzzy parameters, and it depends on the control algorithm used. The fuzzy gains (coefficients of fuzzy rule consequent) u obtained from optimization results (Figs. 13(b)–13(d)) are lower than the initial control surface in Fig. 13(a).

The shapes of control surface have small bumps in the plane of e and Δe for GA-FLC for both mutations and PSO-FLC, and it becomes less distinctive in the ABC-FLC. Also, the control surface by the ABC-FLC is smaller in volume than by the other controllers. However, all control surfaces appear to have the same tendency, which show nonlinear relationship between the gains (u) and fuzzy sets (e and Δe).

5.2. Position control under varying step function

Second task for the drone is to track a reference position in x -direction in terms of varying step function. This type of trajectory is achieved by increasing the position step point from $x = 1$ m to $x = 2$ m at $t = 15$ s. As can be seen from Fig. 14, the drone is stable and responsive, and is also capable of tracking the given varying step function. Controller performances are similar with previous task, where GA-FLC with a mutation rate of 0.1 still has the fastest rise time with the biggest overshoots in every step response. Similarly, ABC-FLC also still has the fastest settling time with the smallest overshoots. Peak time of each controller seems comparable whereas PSO-FLC still appears to be a mediocre controller in terms of control performance. Detail results are further elaborated in Table 7.

Cost functions with respect to number of iterations for each controller are depicted in Fig. 15(a), where the GA-FLC with a mutation rate of 0.1 again shows the premature convergence, and the others converge to certain values as the number of iterations increases. The cost function starts to converge after the-2nd iteration for the PSO-FLC, and after the-4th iteration for the ABC-FLC. However, the ABC-FLC has the best performance compared to the others as indicated by the SSE values in Fig. 15(b). This result reconfirms the advantage of using the ABC-FLC as in the previous section.

Due to the trend of convergence history of the fuzzy sets of e and Δe is similar with previous task, only the initial and tuned fuzzy sets are presented in this section. Initial and tuned fuzzy sets of e and Δe obtained using all control algorithms under varying step function are plotted separately in Fig. 16. As can be seen, the tuned fuzzy sets are also significantly different from the initial fuzzy sets based on the given control algorithms. Similar with previous task, all controllers mostly yield nonuniformity in the shape and the position of fuzzy sets although there are overlap zones among several tuned fuzzy sets. Detail of initial and tuned values are listed in Tables 8–10.

Three-dimensional surfaces for each controller are depicted in Fig. 17. The finding results in previous case are also found in this case. The shapes of control surface have small bumps in the plane of e and Δe for GA-FLC for both mutations and PSO-FLC, and it becomes less distinctive in the ABC-FLC. However, the control surface by the ABC-FLC is smaller in volume than by the other controllers. The control surfaces also appear to have the same tendency, which show nonlinear relationship between the gains (u) and fuzzy sets (e and Δe).

5.3. Position control under sine function

In this section, a daunting task is given to the drone to track a reference position in the x -direction in terms of a sine waveform. This sine function has amplitude of 2 m and frequency of 0.5 Hz. This type of trajectory is usually assigned to circumnavigate a certain object in order to capture visual informations, avoid the obstacles and other applications. The actual position is shown in Fig. 18(a). As can be seen, the GA-FLC with both mutation rates, the PSO-FLC and ABC-FLC have successfully controlled the drone by smoothly tracking the reference position. Quick convergencies have been achieved by all controllers with low cost functions as shown in Figs. 18(b)–18(c), respectively. The main difference among the controllers is the start of convergence of each cost function with respect to the number of iterations. The cost function starts to converge after the-2nd iteration for the GA-FLC with a mutation rate of 0.4 and the ABC-FLC, and after the-3rd iteration for the GA-FLC with a mutation rate of 0.1, and PSO-FLC. However, as the number of iterations increases, the ABC-FLC still has the lowest cost function while the GA-FLC with a mutation rate of 0.1 has still the highest cost function. These results are confirmed by Fig. 18(c).

In order to take a close look at the initial and tuned fuzzy sets of e and Δe obtained using all control algorithms under sine function clearly, the results are plotted separately in Fig. 19. As can be

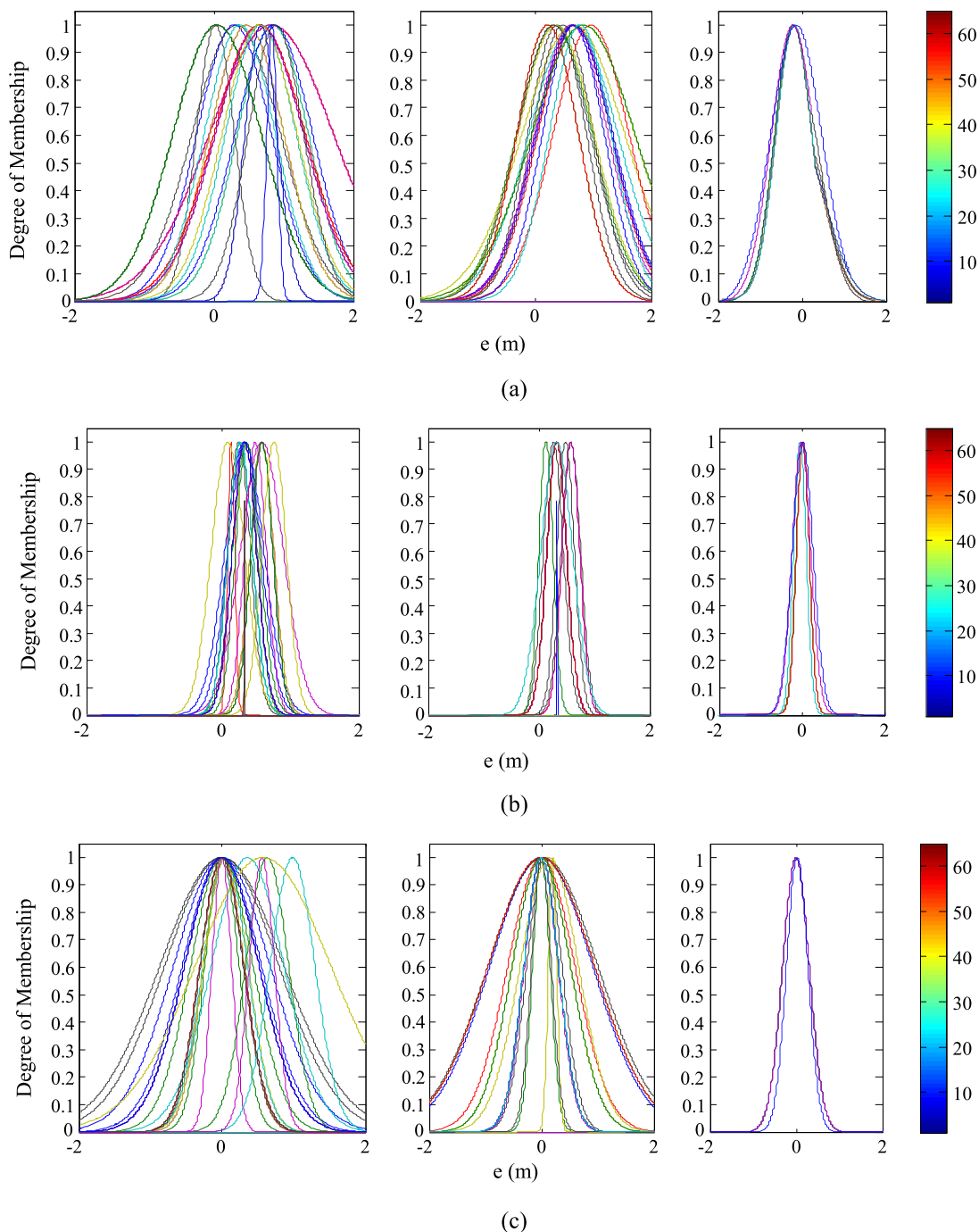


Fig. 11. Convergence histories of fuzzy sets of e for step function in x -axis (a) N (Negative) (b) Z (Zero) (c) P (Positive).

Table 6
Optimal gains of u under step function.

| Gain | Fuzzy set | GA-FLC Mutation rate = 0.1 | | GA-FLC Mutation rate = 0.4 | | PSO-FLC | | ABC-FLC | |
|-------|-----------|-------------------------------|-------|-------------------------------|--------|---------|-------|---------|-------|
| | | Initial | Tuned | Initial | Tuned | Initial | Tuned | Initial | Tuned |
| g_1 | N | 159.96 | 70.08 | 159.96 | 30.02 | 159.96 | 12.13 | 159.96 | 7.5 |
| | | 132.12 | 3.52 | 132.12 | 0.01 | 132.12 | 15.3 | 132.12 | 0.35 |
| | | 103.98 | 0.52 | 103.98 | 10.12 | 103.98 | 0.1 | 103.98 | 0.01 |
| g_1 | Z | 66.34 | 29.1 | 66.34 | 100.06 | 66.34 | 7.1 | 66.34 | 0.5 |
| | | 186.83 | 9.13 | 186.83 | 0.5 | 186.83 | 1.5 | 186.83 | 0.62 |
| | | 49.29 | 0.01 | 49.29 | 0.01 | 49.29 | 0.01 | 49.29 | 0.1 |
| g_1 | P | 102.24 | 220.1 | 102.24 | 55.1 | 102.24 | 50.07 | 102.24 | 16.75 |
| | | 148.06 | 0.14 | 148.06 | 55.03 | 148.06 | 0.1 | 148.06 | 16.12 |
| | | 50.83 | 1.08 | 50.83 | 0.01 | 50.83 | 0.01 | 50.83 | 0.01 |

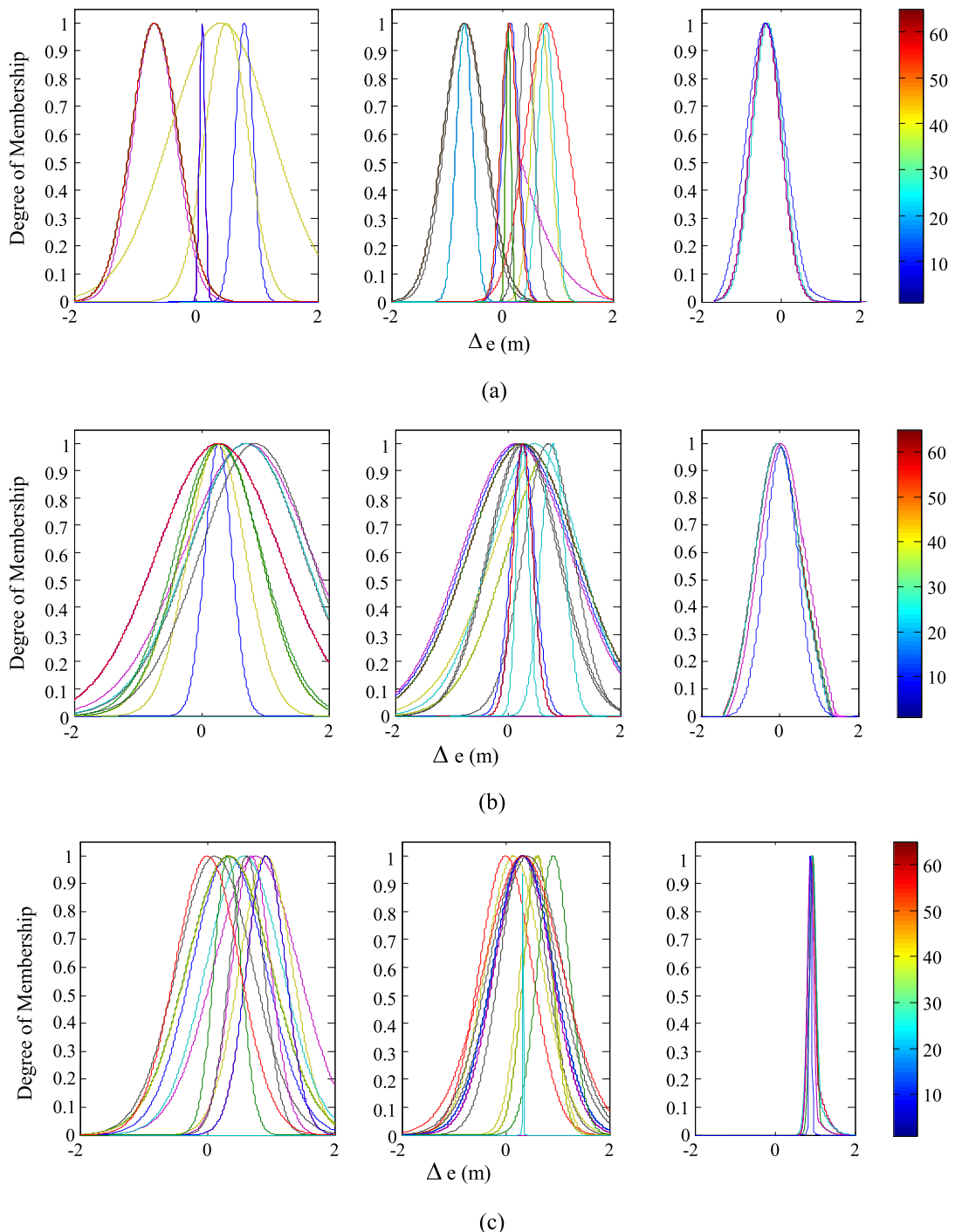


Fig. 12. Convergence histories of fuzzy sets of Δe for step function in x-axis (a) N (Negative) (b) Z (Zero) (c) P (Positive).

Table 7
Controller performance under varying step function.

| Performance | GA-FLC Mutation rate = 0.1 | GA-FLC Mutation rate = 0.4 | PSO-FLC | ABC-FLC |
|-------------------|-------------------------------|-------------------------------|---------|---------|
| Rise time (s) | 14.08 | 14.12 | 14.08 | 14.10 |
| Overshoot (%) | 23.53 | 6.21 | 4.6 | 0.01 |
| Settling time (s) | 16 | 15.54 | 15.37 | 15.18 |
| Peak time (s) | 15.40 | 15.30 | 15.30 | 15.40 |

seen, the initial fuzzy sets are changed based on the given control algorithms. GA-FLC with both mutation rates yield nonuniformity in the shape and position of the fuzzy sets. PSO-FLC controller yields more uniformity than the GA-FLC. In contrary, ABC-FLC

yields the most uniform shape of fuzzy sets among the others, fuzzy sets, and the overlap zone among the tuned fuzzy sets is almost fifty percent.

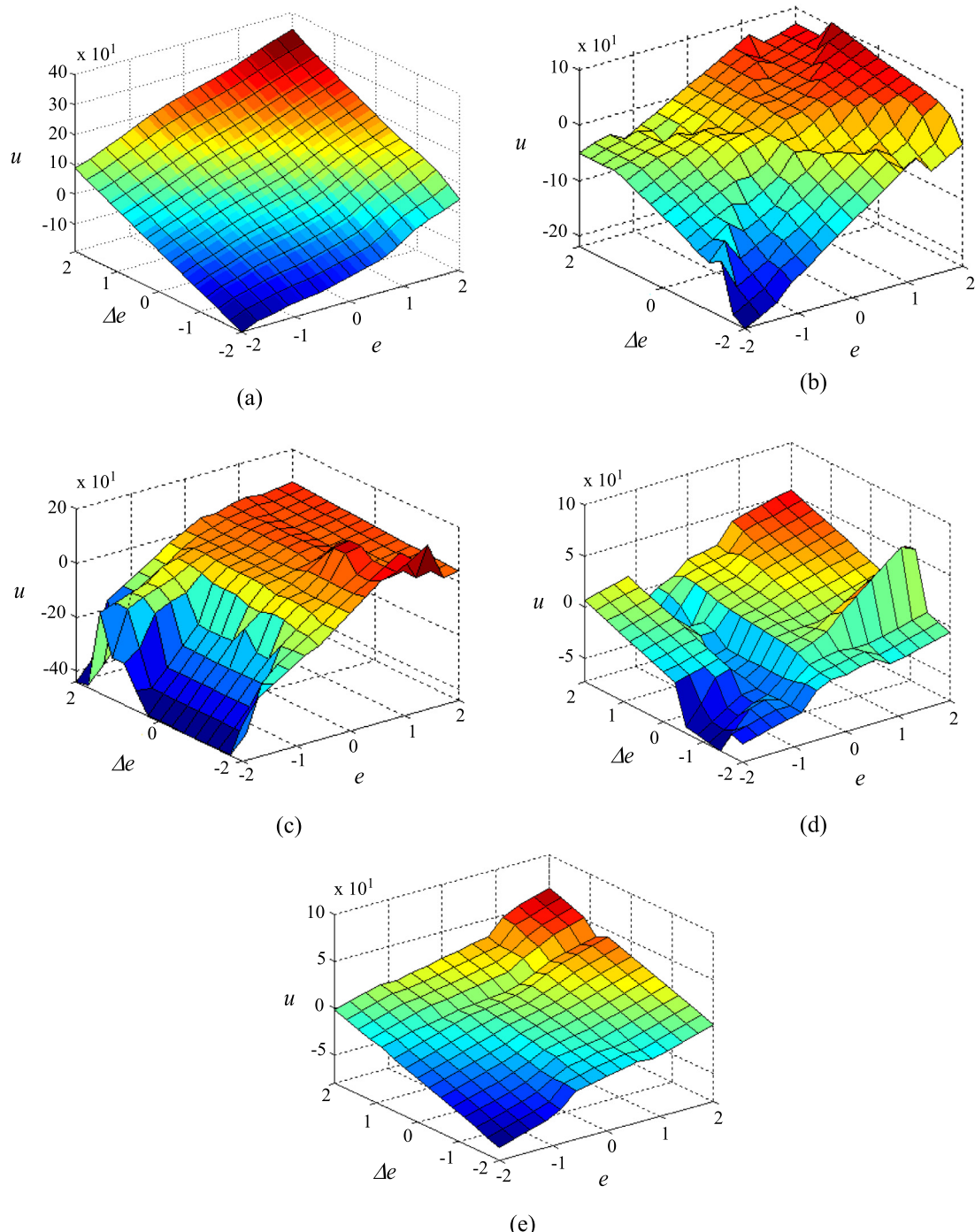


Fig. 13. Three-dimensional surface of FLC for step function in x -direction (a) initial (b) GA-FLC with mutation rate = 0.1 (c) GA-FLC with mutation rate = 0.4 (d) PSO-FLC (e) ABC-FLC.

Table 8

Optimal parameters of membership functions of e under varying step function.

| Parameters | Fuzzy set | GA-FLC | | GA-FLC | | PSO-FLC | | ABC-FLC | |
|------------|-----------|---------------------|-------|---------------------|-------|---------|-------|---------|-------|
| | | Mutation rate = 0.1 | | Mutation rate = 0.4 | | Initial | Tuned | Initial | Tuned |
| | | Initial | Tuned | Initial | Tuned | Initial | Tuned | Initial | Tuned |
| σ | N | 0.52 | 0.1 | 0.52 | 0.3 | 0.52 | 0.08 | 0.52 | 0.18 |
| | | 0.17 | -1.12 | 0.17 | -0.42 | 0.17 | -0.6 | 0.17 | -0.2 |
| σ | Z | 0.19 | 0.5 | 0.19 | 0.08 | 0.19 | 0.08 | 0.19 | 0.2 |
| | | 0.007 | 0.01 | 0.007 | 0.01 | 0.007 | 0 | 0.007 | 0 |
| σ | P | 0.05 | 0.5 | 0.05 | 0.4 | 0.05 | 0.08 | 0.05 | 0.1 |
| | | -0.88 | 1.2 | -0.88 | 0.63 | -0.88 | 0.5 | -0.88 | 0.2 |

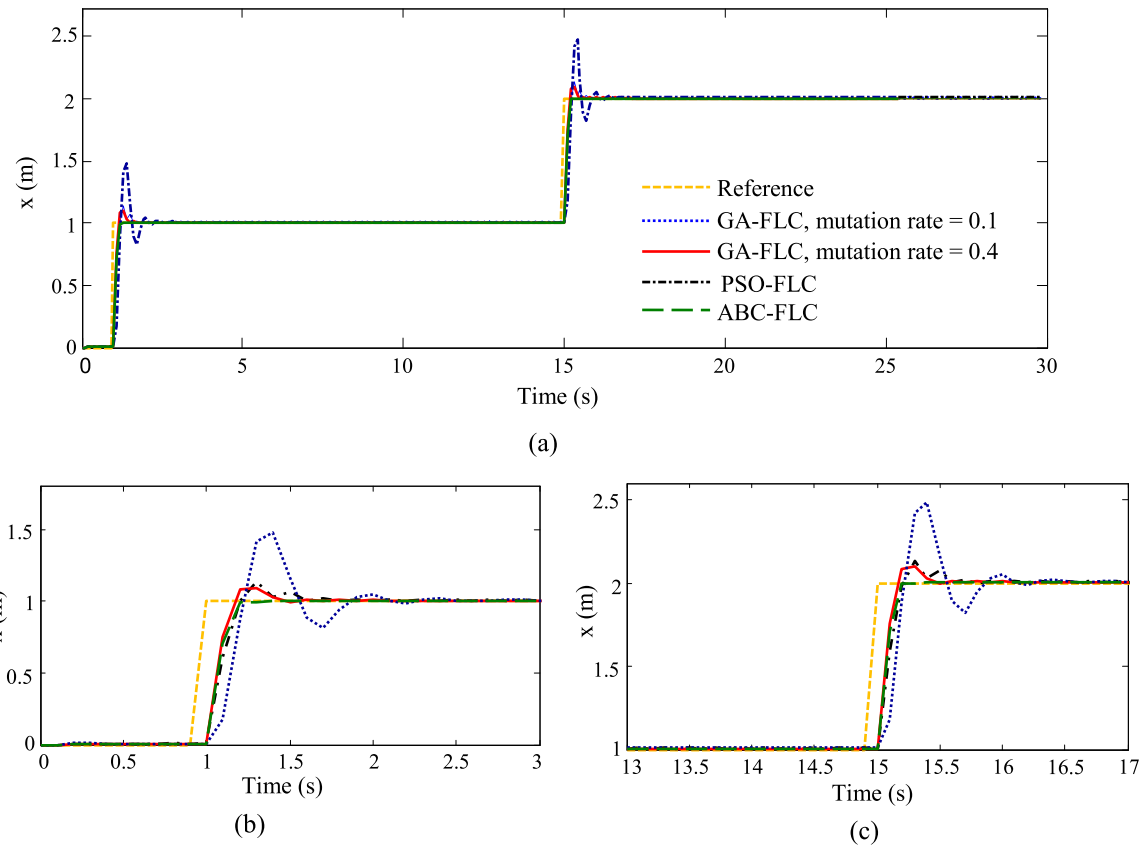


Fig. 14. Drone response for varying step function in x -direction (a) time window of 0–30 s (b) time window of 0–3 s (c) time window of 13–17 s.

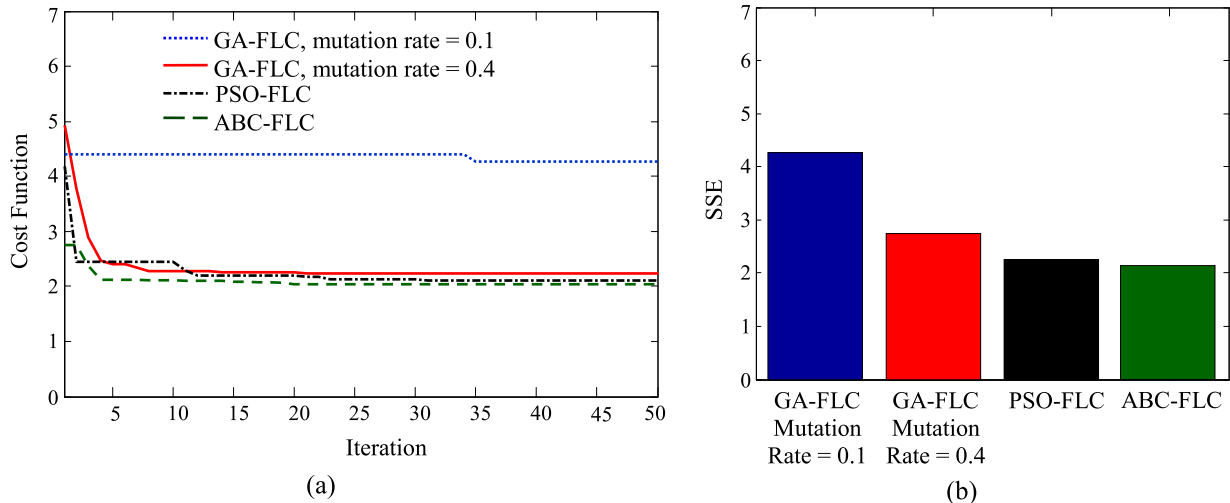


Fig. 15. Cost functions for varying step function in x -direction (a) cost function with respect to number of iterations (b) SSE.

Table 9
Optimal parameters of membership functions of Δe under varying step function.

| Parameters | Fuzzy set | GA-FLC Mutation rate = 0.1 | | GA-FLC Mutation rate = 0.4 | | PSO-FLC | | ABC-FLC | |
|------------|-----------|----------------------------|-------|----------------------------|-------|---------|-------|---------|-------|
| | | | | | | | | | |
| | | Initial | Tuned | Initial | Tuned | Initial | Tuned | Initial | Tuned |
| σ | N | 0.33 | 0.08 | 0.33 | 0.25 | 0.33 | 0.08 | 0.33 | 0.21 |
| | | 0.26 | -1.1 | 0.26 | -0.86 | 0.26 | -0.17 | 0.26 | -0.5 |
| σ | Z | 0.89 | 0.5 | 0.89 | 0.13 | 0.89 | 0.08 | 0.89 | 0.08 |
| | | 0.35 | 0.01 | 0.35 | 0.01 | 0.35 | 0 | 0.35 | 0 |
| σ | P | 0.68 | 0.08 | 0.68 | 0.25 | 0.68 | 0.08 | 0.68 | 0.08 |
| | | 0.39 | 1.08 | 0.39 | 0.91 | 0.39 | 0.32 | 0.39 | 0.9 |

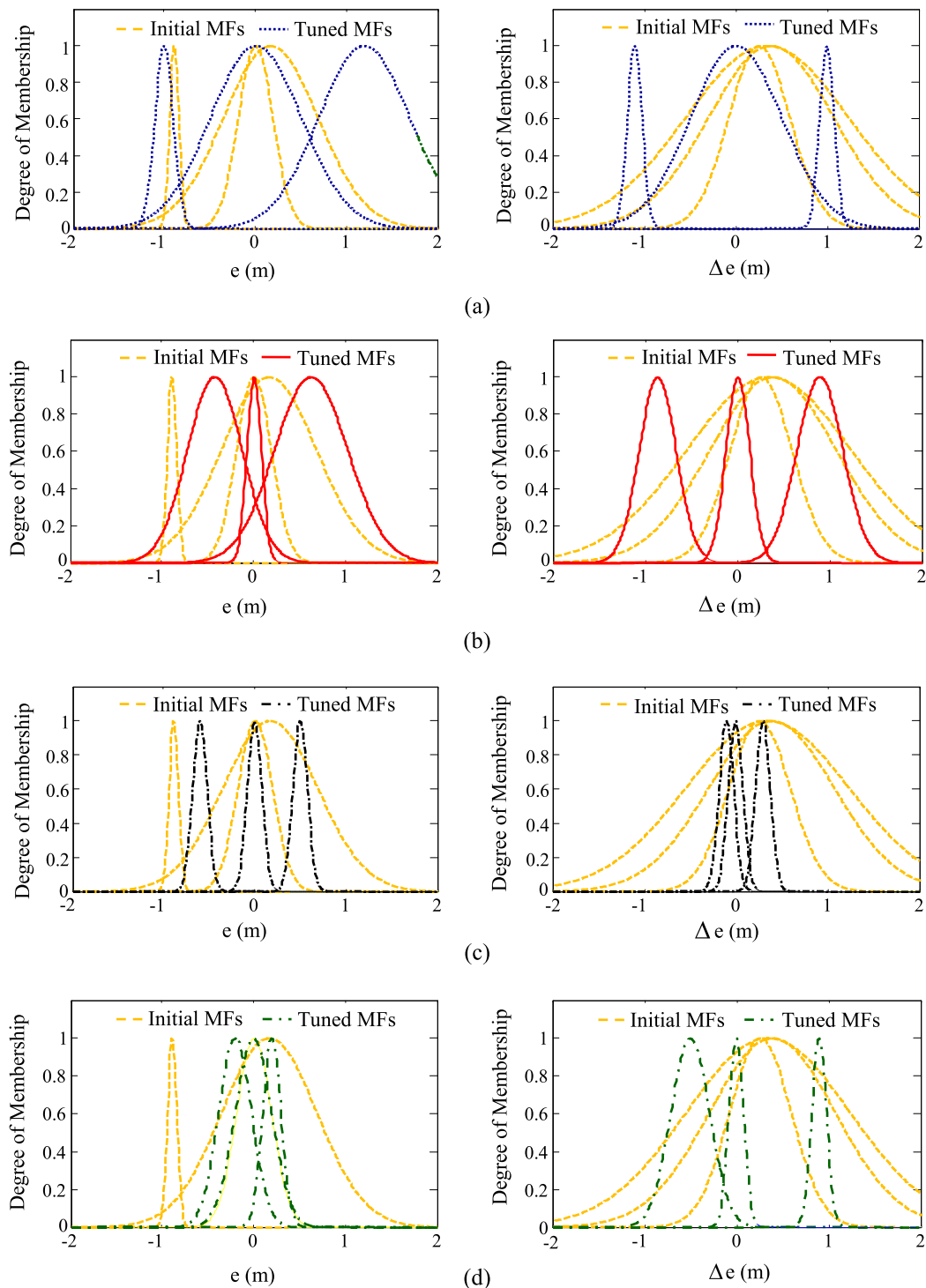


Fig. 16. Initial and tuned fuzzy sets of e and Δe for varying step function in x -axis (a) GA-FLC with mutation rate = 0.1 (b) GA-FLC with mutation rate = 0.4 (c) PSO-FLC (d) ABC-FLC.

By utilizing the data in Tables 11–13, three-dimensional surfaces of each controller can be plotted and shown in Fig. 20. It is found that the control surfaces tuned from control algorithms are different with the initial control surface. It is seen that they are affected significantly by the values of tuned fuzzy parameters. The shapes of control surface have small bumps in the plane of e and Δe , and it becomes more distinctive in the ABC-FLC. Also, the control surface by the ABC-FLC is smaller in volume than by the other controllers like the two previous cases. However, all control surfaces appear to have the same tendency, which is nonlinear.

6. Conclusions and suggestions

Evolutionary algorithms-based self-tuning of the first-order Takagi-Sugeno-Kang-type fuzzy logic controller (FLC) are proposed. The proposed controllers are applied for the trajectory tracking of a quadcopter drone. Several important finding results and suggestions from this work are listed as follows:

- Given constant and varying step functions, ABC-FLC has slower rise and peak time, and faster settling time in the

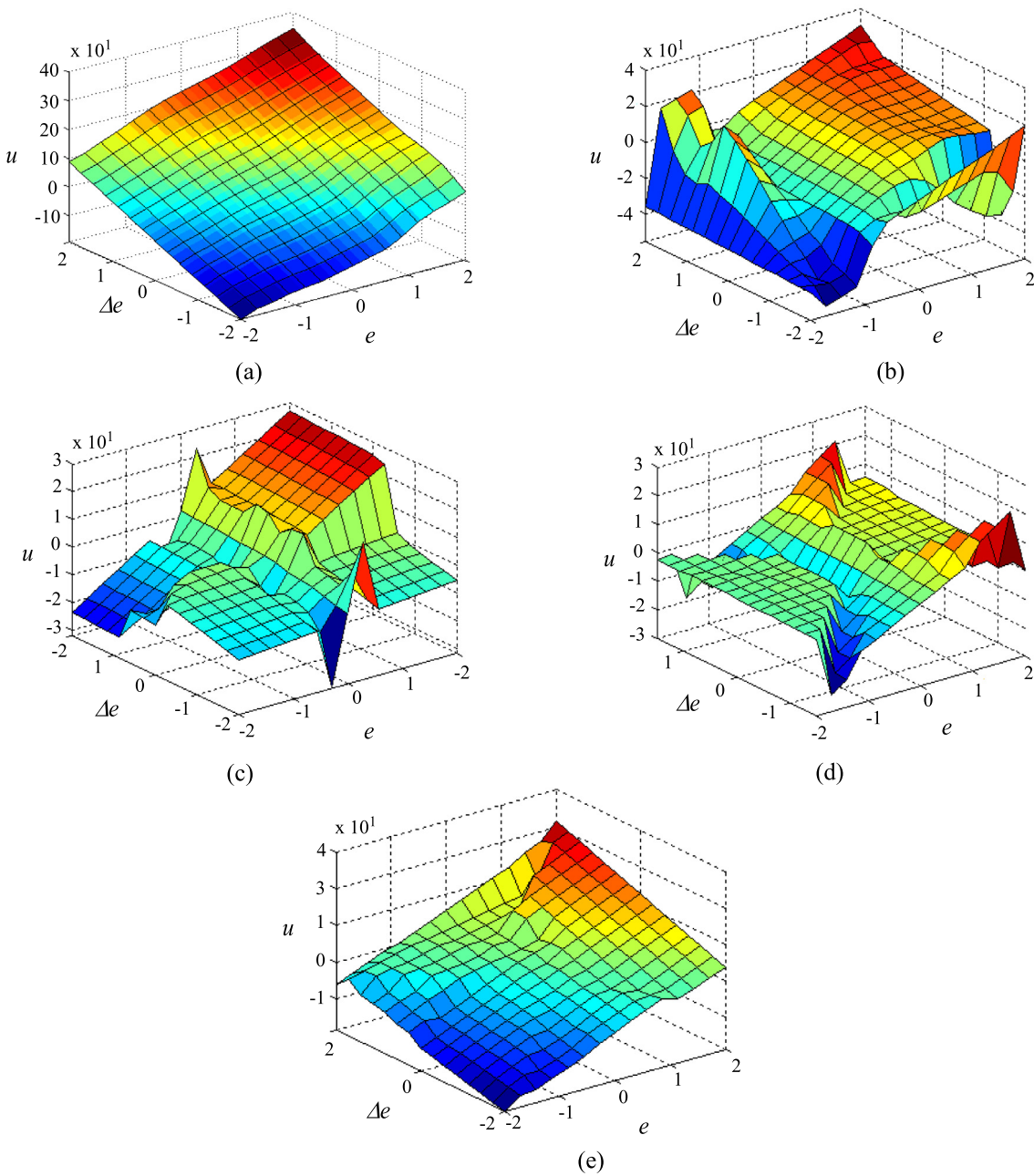


Fig. 17. Three-dimensional surface of FLC for varying step function in x -direction (a) initial (b) GA-FLC with mutation rate = 0.1 (c) GA-FLC with mutation rate = 0.4 (d) PSO-FLC (e) ABC-FLC.

Table 10
Optimal gains of u under varying step function.

| Gain | Fuzzy set | GA-FLC Mutation rate = 0.1 | | GA-FLC Mutation rate = 0.4 | | PSO-FLC | | ABC-FLC | |
|-------|-----------|-------------------------------|-------|-------------------------------|-------|---------|-------|---------|-------|
| | | Initial | Tuned | Initial | Tuned | Initial | Tuned | Initial | Tuned |
| g_1 | N | 159.96 | 6.1 | 159.96 | 12.8 | 159.96 | 2.03 | 159.96 | 1.01 |
| | | 132.12 | 5.06 | 132.12 | 0.85 | 132.12 | 0.9 | 132.12 | 0.5 |
| | | 103.98 | 0.1 | 103.98 | 0.1 | 103.98 | 0.25 | 103.98 | 0.001 |
| g_1 | Z | 66.34 | 19.11 | 66.34 | 25.13 | 66.34 | 26.17 | 66.34 | 6.31 |
| | | 186.83 | 1.02 | 186.83 | 1.41 | 186.83 | 0.41 | 186.83 | 4.42 |
| | | 49.29 | 0.01 | 49.29 | 0.12 | 49.29 | 0.27 | 49.29 | 0.11 |
| g_1 | P | 102.24 | 1.14 | 102.24 | 1.71 | 102.24 | 1.08 | 102.24 | 6.24 |
| | | 148.06 | 32.09 | 148.06 | 4.53 | 148.06 | 0.9 | 148.06 | 1.9 |
| | | 50.83 | 0.01 | 50.83 | 0.01 | 50.83 | 0.12 | 50.83 | 0 |

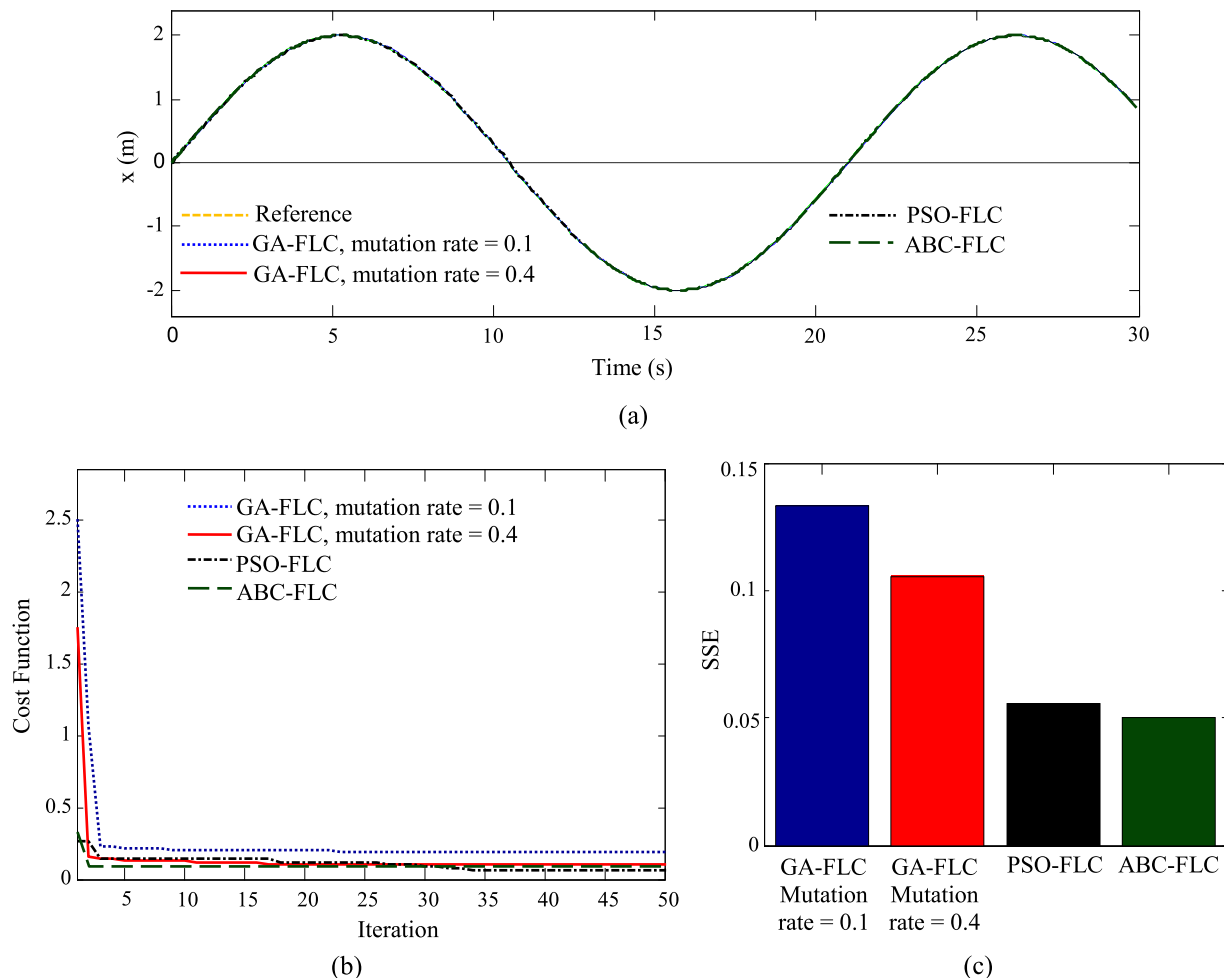


Fig. 18. Position control under sine function in x -direction (a) drone response (b) cost function with respect to number of iterations (c) SSE.

Table 11
Optimal parameters of membership functions of e under sine function.

| Parameters | Fuzzy set | GA-FLC Mutation rate = 0.1 | | GA-FLC Mutation rate = 0.4 | | PSO-FLC | | ABC-FLC | |
|------------|-----------|----------------------------|-------|----------------------------|-------|---------|-------|---------|-------|
| | | Initial | Tuned | Initial | Tuned | Initial | Tuned | Initial | Tuned |
| σ | N | 0.52 | 0.6 | 0.52 | 0.08 | 0.52 | 0.2 | 0.52 | 0.12 |
| c | | 0.17 | -0.2 | 0.17 | -0.6 | 0.17 | -1.2 | 0.17 | -0.4 |
| σ | Z | 0.19 | 0.25 | 0.19 | 0.17 | 0.19 | 0.2 | 0.19 | 0.08 |
| c | | 0.007 | 0.03 | 0.007 | 0.01 | 0.007 | 0.01 | 0.007 | -0.01 |
| σ | P | 0.05 | 0.3 | 0.05 | 0.5 | 0.05 | 0.11 | 0.05 | 0.1 |
| c | | -0.88 | 0.2 | -0.88 | 0.9 | -0.88 | 1.2 | -0.88 | 0.4 |

Table 12
Optimal parameters of membership functions of Δe under sine function.

| Parameters | Fuzzy set | GA-FLC Mutation rate = 0.1 | | GA-FLC Mutation rate = 0.4 | | PSO-FLC | | ABC-FLC | |
|------------|-----------|----------------------------|-------|----------------------------|-------|---------|-------|---------|-------|
| | | Initial | Tuned | Initial | Tuned | Initial | Tuned | Initial | Tuned |
| σ | N | 0.33 | 0.6 | 0.33 | 0.08 | 0.33 | 0.1 | 0.33 | 0.1 |
| c | | 0.26 | -0.4 | 0.26 | -0.1 | 0.26 | -1.05 | 0.26 | -0.3 |
| σ | Z | 0.89 | 0.4 | 0.89 | 0.5 | 0.89 | 0.21 | 0.89 | 0.1 |
| c | | 0.35 | 0.01 | 0.35 | 0.01 | 0.35 | 0.4 | 0.35 | 0.01 |
| σ | P | 0.68 | 0.03 | 0.68 | 0.08 | 0.68 | 0.1 | 0.68 | 0.1 |
| c | | 0.39 | 0.9 | 0.39 | 0.7 | 0.39 | 1.11 | 0.39 | 0.1 |

absence of overshoots. On the contrary, GA-FLC with mutation rate of 0.1 has faster rise time and bigger overshoots compared to GA-FLC with a mutation rate of 0.4 and PSO-FLC.

- For cost functions under constant step function, PSO-FLC and GA-FLC with mutation rate of 0.4 converge faster than the ABC-FLC and GA-FLC with a mutation rate of 0.4. However, ABC-FLC has the lowest cost function among other

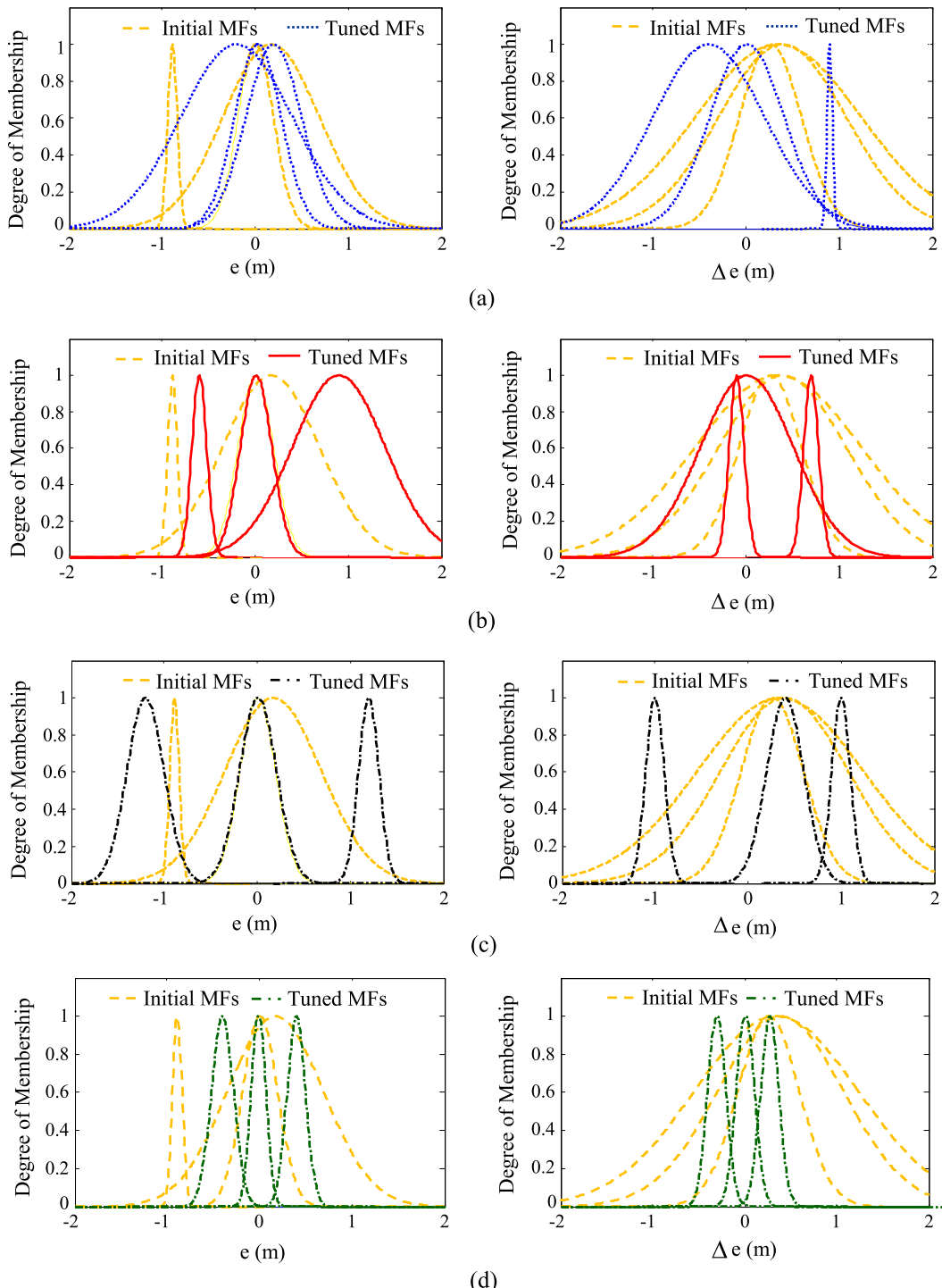


Fig. 19. Initial and final fuzzy sets of e and Δe for sine function in x -axis (a) GA-FLC with mutation rate = 0.1 (b) GA-FLC with mutation rate = 0.4 (c) PSO-FLC (d) ABC-FLC.

controllers. Under varying step functions, GA-FLC with a mutation rate of 0.1 exhibits premature convergence, and PSO-FLC appears to be the fastest convergence.

- Overall, the convergence histories of the fuzzy sets of ABC-FLC show that in the beginning of iteration, the values of c and σ are largely scattered so that the shape and position of the fuzzy sets are ununiform. As the number of iterations increases, the values of c and σ converge and, the shape and position of the fuzzy sets are getting localized in certain values. The patterns are similar for GA-FLC and PSO-FLC.

- Given constant and varying step functions, all proposed controllers yield ununiformity in the shape and the position of fuzzy sets although there are overlap zones among several tuned fuzzy sets. However, under sine function, ABC-FLC yields the most uniform shape of fuzzy sets among other controllers, and the overlap zone among the tuned fuzzy sets is almost fifty percent.
- Overall, all three-dimensional control surfaces appear to have the same tendency, which is nonlinear while the volume of the ABC-FLC is smaller than the other controllers. However, under constant and varying step functions, the

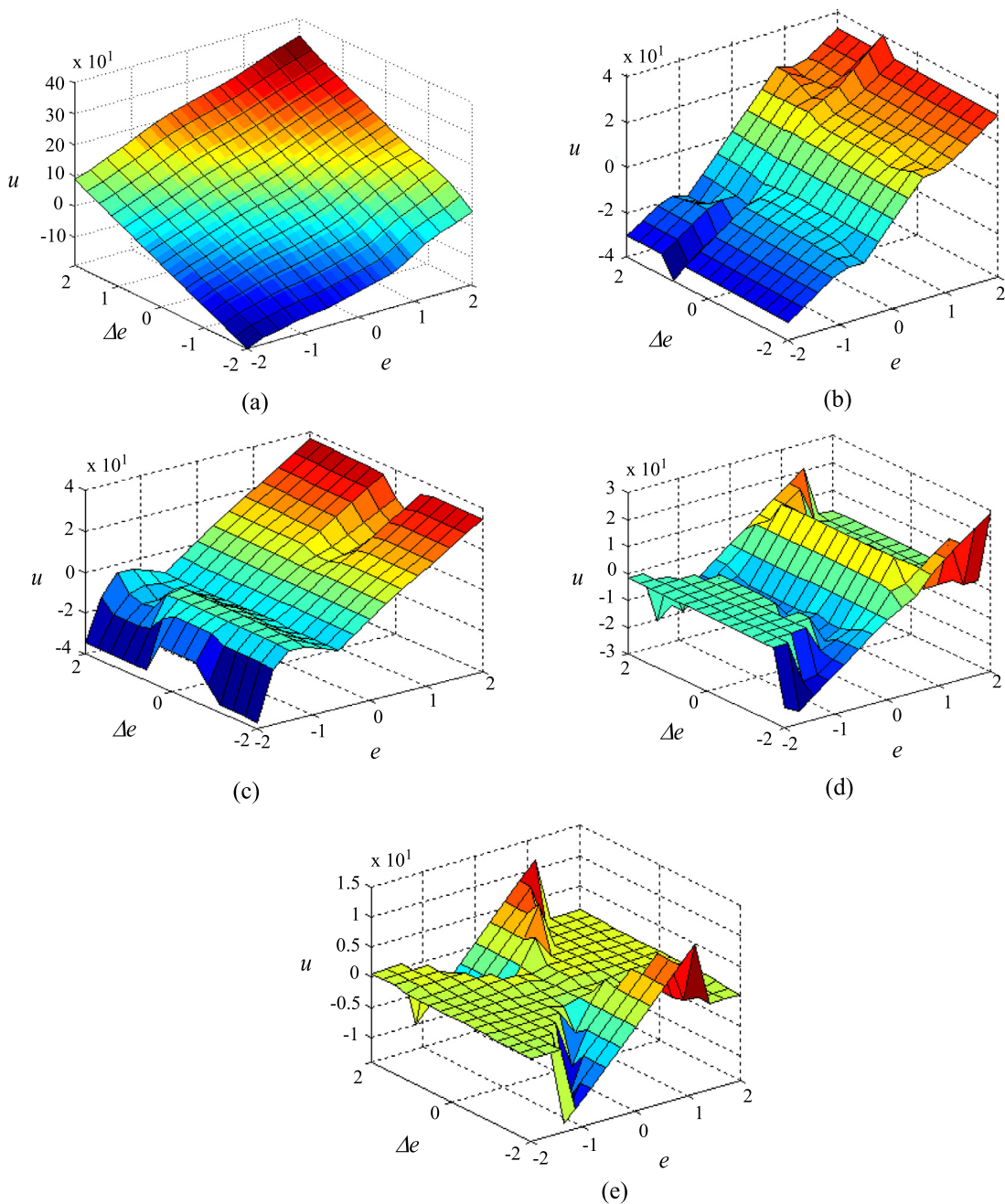


Fig. 20. Three-dimensional control surface of FLC for sine function in x -direction (a) initial (b) GA-FLC with mutation rate = 0.1 (c) GA-FLC with mutation rate = 0.4 (d) PSO-FLC (e) ABC-FLC.

Table 13
Optimal gains of u under sine function.

| Gain | Fuzzy set | GA-FLC Mutation rate = 0.1 | | GA-FLC Mutation rate = 0.4 | | PSO-FLC | | ABC-FLC | |
|-------|-----------|-------------------------------|-------|-------------------------------|-------|---------|-------|---------|-------|
| | | Initial | Tuned | Initial | Tuned | Initial | Tuned | Initial | Tuned |
| g_1 | N | 159.96 | 28.8 | 159.96 | 17.82 | 159.96 | 1.13 | 159.96 | 0.1 |
| g_2 | | 132.12 | 0.18 | 132.12 | 0.65 | 132.12 | 0.1 | 132.12 | 0.01 |
| b | | 103.98 | 0.02 | 103.98 | 0.02 | 103.98 | 0.01 | 103.98 | 0.8 |
| g_1 | Z | 66.34 | 46.50 | 66.34 | 20.5 | 66.34 | 28.02 | 66.34 | 28.07 |
| g_2 | | 186.83 | 0.87 | 186.83 | 0.1 | 186.83 | 0.1 | 186.83 | 0.1 |
| b | | 49.29 | 0.087 | 49.29 | 0.15 | 49.29 | 0.01 | 49.29 | 0.05 |
| g_1 | P | 102.24 | 15.65 | 102.24 | 3.05 | 102.24 | 1.08 | 102.24 | 0.1 |
| g_2 | | 148.06 | 0.34 | 148.06 | 0.35 | 148.06 | 0.1 | 148.06 | 0.001 |
| b | | 50.83 | 0.94 | 50.83 | 0.1 | 50.83 | 0.01 | 50.83 | 0 |

shapes of the control surface of the ABC-FLC has less distinctive small bumps in the plane of e and Δe , while under the case of sine function, the ABC-FLC has distinctive smaller bumps compared to other controllers.

- The gains of proposed controllers g_{1k} , g_{2k} and b_k are fixed. However, it can easily be extended to time-variant. The system is transferable to the Mamdani type FLC, where the consequents are in the form of fuzzy sets.
- The application of the proposed controllers is not only limited to the quadcopter drone, but also to other dynamic systems.
- Future works should include tuning the suitable number of fuzzy sets and T-S-K satisfying the required robust performances.
- Other nature-inspired metaheuristic algorithms based FLC such as Ant Colony, Cuckoo Search, Differential Evolution, and Gray Wolf algorithms are very potential to be applied. However, they are not yet implemented at this phase of study and can be recommended as our potential future directions.

Acknowledgments

Financial support of this work from the Indonesian Institute of Sciences, Indonesia and experimental work from University of New South Wales, Australia are gratefully appreciated.

References

- [1] L.A. Zadeh, Fuzzy Sets, *Inf. Control* 8 (3) (1965) 338–353.
- [2] E.H. Mamdani, Advances in the linguistic synthesis of fuzzy controllers, *Int. J. Man-Mach. Stud.* 8 (6) (1976) 669–678.
- [3] T. Takagi, M. Sugeno, Fuzzy Identification of systems and its applications to modelling and control, *IEEE Trans. Syst. Man Cybern. smc-15* (1) (1985) 116–132.
- [4] M. Sugeno, G.T. Kang, Structure identification of fuzzy model, *Fuzzy Sets and Systems* 28 (1) (1988) 15–33.
- [5] H.K. Lam, A review on stability analysis of continuous time fuzzy model based control systems: From membership function independent to membership function dependent analysis, *Eng. Appl. Artif. Intell.* 67 (2018) 390–408.
- [6] M. Mokarram, A. Khoei, K. Hadidi, CMOS Fuzzy logic controller supporting fractional polynomial membership functions, *Fuzzy Sets and Systems* 263 (2015) 112–126.
- [7] S.Y. Wang, F.Y. Liu, J.H. Chou, Adaptive TSK fuzzy sliding mode control design for switched reluctance motor DTC drive systems with torque sensorless strategy, *Appl. Soft Comput.* 66 (2018) 278–291.
- [8] A. Kumar, V. Kumar, A novel interval type-2 fractional order fuzzy PID controller: Design, performance evaluation, and its optimal time domain tuning, *ISA Trans.* 68 (2017) 251–275.
- [9] J. Smocek, J. Spytko, Evolutionary algorithm-based design of a TBF predictive model and TSK fuzzy anti-sway crane control system, *Eng. Appl. Artif. Intell.* 28 (2014) 190–200.
- [10] O.N. Almasi, V. Fereshtehpoor, M.H. Khooban, F. Blaabjerg, Analysis, control and design of a non-inverting buck-boost converter: A bump-less two level T-S fuzzy PI control, *ISA Trans.* 67 (2017) 515–527.
- [11] I. Boulkaibet, K. Belarbi, S. Bououden, T. Marwala, M. Chadli, A new T-S fuzzy model predictive control for nonlinear process, *Expert Syst. Appl.* 88 (2017) 132–151.
- [12] A.J.H.A. Gizi, M.W. Mustafa, N.A. Al-geelani, M.A. Aksaedi, Sugeno fuzzy PID tuning, by genetic-neutral for AVR in electrical power generation, *Appl. Soft Comput.* 28 (2015) 226–236.
- [13] X. Sun, H. Zhang, J. Han, Y. Wang, Non-fragile for interval type-2 TSK fuzzy logic control systems with-delay, *J. Franklin Inst. B* 354 (2017) 7997–8014.
- [14] S. Yordanova, M. Slavov, B. Gueorguiev, Parallel distributed compensation for improvement of level control in carbonization column for soda production, *Expert Syst. Appl.* 71 (2018) 53–60.
- [15] O. Castillo, L.A. Angulo, J.R. Castro, M.G. Valdez, A comparative study of type-1 fuzzy logic systems, interval type-2 fuzzy logic systems and generalized type-2 fuzzy logic systems in control problems, *Inf. Sci.* 354 (2016) 257–274.
- [16] N.D. Zoric, A.M. Simonovic, Z.S. Mitrovic, S.N. Stupar, A.M. Obradovic, N.S. Lukic, Free vibration control of smart composite beams using particle swarm optimized self-tuning fuzzy logic controller, *J. Sound Vib.* 333 (2014) 5244–5268.
- [17] S.H. Tsai, Y.W. Chen, A novel identification method for Takagi-Sugeno fuzzy model, *Fuzzy Sets and Systems* 338 (2018) 117–135.
- [18] R.E. Precup, M.C. Sabau, E.M. Petriu, Nature-inspired optimal tuning of input membership functions of Takagi-Sugeno-Kang fuzzy models for anti-lock braking systems, *Appl. Soft Comput.* 27 (2015) 575–589.
- [19] R.E. Precup, H.I. Filip, M.B. Radac, E.M. Petriu, S. Preitl, C.A. Dragos, Online identification of evolving Takagi-Sugeno-Kang fuzzy models for crane systems, *Appl. Soft Comput.* 24 (2014) 1155–1163.
- [20] P.C. Chang, J.L. Wu, J.J. Lin, A takagi-sugeno fuzzy model combined with a support vector regression for stock trading forecasting, *Appl. Soft Comput.* 38 (2016) 831–842.
- [21] S.H. Tsai, Y.W. Chen, A novel identification method for Takagi-Sugeno fuzzy model, *Fuzzy Sets and Systems* 338 (2018) 117–135.
- [22] M.S. Shokouhifar, A. Jalali, Optimized sugeno fuzzy clustering algorithm for wireless sensor networks, *Eng. Appl. Artif. Intell.* 60 (2017) 16–25.
- [23] F. Santoso, M.A. Garrat, S.G. Anavatti, Fuzzy logic-based self-tuning autopilots for trajectory tracking of a low-cost quadcopter: a comparative study, in: Proc. of the 4th International Conference on Soft Computing for Problem Solving, 2014, pp. 53–65.
- [24] D.E. Goldberg, *Genetic Algorithms in Search, Optimization, and Machine Learning*, first ed., Addison-Wesley Professional, 1989.
- [25] A. Machmudah, S. Parman, A. Zainuddin, S. Chacko, Polynomial joint angle arm robot motion planning in complex geometrical obstacles, *Appl. Soft Comput.* 13 (2013) 1099–1109.
- [26] E. Yazid, E.M.S. Liew, S. Parman, V.J. Kurian, Improving the modelling capacity of Volterra model using evolutionary computing methods based on Kalman Smoother adaptive filter, *Appl. Soft Comput.* 35 (2015) 695–707.